Received: 18 January 2023 | Revised: 21 February 2024 | Accepted: 18 March 2024

DOI: 10.1111/bph.16390

RESEARCH ARTICLE

Identification and characterisation of functional $K_{ir}6.1$-containing ATP-sensitive potassium channels in the cardiac ventricular sarcolemmal membrane

Sean Brennan[1] | Shen Chen[2] | Samir Makwana[2] | Simona Esposito[1,2] | Lauren R. McGuinness[1] | Abrar I. M. Alnaimi[1,3] | Mark W. Sims[2] | Manish Patel[2] | Qadeer Aziz[4] | Leona Ojake[4] | James A. Roberts[1] | Parveen Sharma[1] | David Lodwick[2] | Andrew Tinker[4] | Richard Barrett-Jolley[5] | Caroline Dart[6] | Richard D. Rainbow[1]

[1]Department of Cardiovascular and Metabolic Medicine and Liverpool Centre for Cardiovascular Science, University of Liverpool, Liverpool, UK

[2]Department of Cardiovascular Sciences, University of Leicester, Leicester, UK

[3]Department of Cardiac Technology, Imam Abdulrahman Bin Faisal University, Dammam, Saudi Arabia

[4]William Harvey Research Institute, Queen Mary University of London, London, UK

[5]Department of Musculoskeletal and Ageing Science, University of Liverpool, Liverpool, UK

[6]Department of Biochemistry, Cell and Systems Biology, University of Liverpool, Liverpool, UK

Correspondence
Richard Rainbow, Department of Cardiovascular and Metabolic Medicine and Liverpool Centre for Cardiovascular Sciences, Institute of Life Course and Medical Sciences, University of Liverpool, William Henry Duncan Building, 6 West Derby Street, Liverpool, Merseyside, L7 8TX, UK.
Email: richard.rainbow@liverpool.ac.uk

Funding information
British Heart Foundation, Grant/Award Numbers: FS/PhD/21/29165, PG/16/14/32039, PG/19/18/34280; Wellcome Trust, Grant/Award Number: 204822/Z/16/Z; Faculty of Health and Life

Abstract

Background and Purpose: The canonical $K_{ir}6.2$/SUR2A ventricular K_{ATP} channel is highly ATP-sensitive and remains closed under normal physiological conditions. These channels activate only when prolonged metabolic compromise causes significant ATP depletion and then shortens the action potential to reduce contractile activity. Pharmacological activation of K_{ATP} channels is cardioprotective, but physiologically, it is difficult to understand how these channels protect the heart if they only open under extreme metabolic stress. The presence of a second K_{ATP} channel population could help explain this. Here, we characterise the biophysical and pharmacological behaviours of a constitutively active $K_{ir}6.1$-containing K_{ATP} channel in ventricular cardiomyocytes.

Experimental Approach: Patch-clamp recordings from rat ventricular myocytes in combination with well-defined pharmacological modulators was used to characterise these newly identified K^+ channels. Action potential recording, calcium (Fluo-4) fluorescence measurements and video edge detection of contractile function were used to assess functional consequences of channel modulation.

Key Results: Our data show a ventricular K^+ conductance whose biophysical characteristics and response to pharmacological modulation were consistent with $K_{ir}6.1$-containing channels. These $K_{ir}6.1$-containing channels lack the ATP-sensitivity of the canonical channels and are constitutively active.

Conclusion and Implications: We conclude there are two functionally distinct populations of ventricular K_{ATP} channels: constitutively active $K_{ir}6.1$-containing channels

Abbreviations: APD, action potential duration; APD_{90}, action potential to 90% repolarised; CiPA, Comprehensive in vitro Proarrhythmia Assay; K_{ATP} Channel, ATP sensitive potassium channel; KCNJ8 KD, KCNJ8 (Kir6.1) knockdown; SUR, sulfonylurea receptor.

Sean Brennan and Shen Chen contributed equally to this work.

Sciences, University of Liverpool; University of Leicester

that play an important role in fine-tuning the action potential and $K_{ir}6.2$/SUR2A channels that activate with prolonged ischaemia to impart late-stage protection against catastrophic ATP depletion. Further research is required to determine whether $K_{ir}6.1$ is an overlooked target in Comprehensive in vitro Proarrhythmia Assay (CiPA) cardiac safety screens.

KEYWORDS
ATP-sensitive potassium channel, cardiomyocytes, K_{ATP} channels, Kir6.1

1 | INTRODUCTION

Our current understanding of the canonical adenosine triphosphate (ATP)-sensitive potassium (K_{ATP}) channels in the heart suggests that they should be electrically silent under normal physiological conditions, but open in response to severe ischaemia to protect the heart from damage. These integral membrane proteins are inhibited by ATP and activated by Mg^{2+}-bound nucleotides and thus translate changes in metabolism to changes in membrane K^+ permeability and cellular excitability (reviewed by Nichols, 2006; Tinker et al., 2018). Functional K_{ATP} channels form as octamers of four $K_{ir}6$ pore-forming K^+ channel subunits and four sulphonylurea receptor (SUR) subunits (Li, Wu, et al., 2017; Martin et al., 2017). Two $K_{ir}6$ subunits, **$K_{ir}6.1$** and **$K_{ir}6.2$**, have been identified, encoded by *KCNJ8* and *KCNJ11*, respectively (Inagaki, Gonoi, et al., 1995; Inagaki, Tsuura, et al., 1995) and two SUR genes are known, **ABCC8 (SUR1)** and **ABCC9 (SUR2)**, the latter giving rise to SUR2A and SUR2B by alternative splicing (Aguilar-Bryan et al., 1995; Chutkow et al., 1996). $K_{ir}6$ and SUR2 subunits are well conserved across species with a reported 95%–97% sequence homology across human, rat, mouse and rabbit (Brochiero et al., 2002; Inagaki, Gonoi et al., 1995; Sung et al., 2021). The molecular make-up of individual channels within tissues is complicated by evidence that the different $K_{ir}6$ and SUR subunits can come together in any combination to form functional channels with different regulatory properties and sensitivity to ATP (Akrouh et al., 2009; Brennan et al., 2020; Lodwick et al., 2014).

The accepted view is that highly ATP-sensitive $K_{ir}6.2$/SUR2A channels predominate in the heart (Nichols, 2016), although $K_{ir6}.1$, $K_{ir}6.2$, SUR1, SUR2A and SUR2B have all been shown to be expressed at the sarcolemmal surface of the sinoatrial node (Aziz et al., 2014; D'Souza et al., 2014), atrial (D'Souza et al., 2014; Flagg et al., 2008) or of ventricular cardiomyocytes (Aziz et al., 2014, 2017; Morrissey, Parachuru, et al., 2005; Morrissey, Rosner, et al., 2005; Singh et al., 2003). Although inactive under normal physiological conditions due to ATP inhibition (Inagaki, Gonoi et al., 1995; Inagaki, Tsuura et al., 1995; Inagaki et al., 1996), ventricular $K_{ir}6.2$/SUR2A channels open during severe metabolic stress (Brennan et al., 2015, 2019; Noma, 1983), causing shortening of the action potential (AP) and reduction of Ca^{2+} entry, and so a reduced contractile activity as crucial energy-sparing protective mechanisms (Brennan et al., 2015; Cole et al., 1991; Nichols, 2016; Suzuki et al., 2002).

What is already known

- The accepted view is that highly ATP-sensitive $K_{ir}6.2$/SUR2A (K_{ATP}) channels functionally dominate in ventricular cardiomyocytes.
- Due to their ATP sensitivity, cardiac $K_{ir}6.2$/SUR2A channels cannot open until catastrophic intracellular ATP depletion.

What does this study add

- We characterise cell-surface ventricular channels that are biophysically, pharmacologically and genetically identical to $K_{ir}6.1$-containing channels.
- These $K_{ir}6.1$-containing K_{ATP} channels are constitutively active, modulating action potential duration and excitation–contraction coupling.

What is the clinical significance

- Cardiac safety screening is vital in drug discovery; the CiPA initiative screens various ion channels.
- The modulation of ventricular action potentials by $K_{ir}6.1$ suggests this may need to be screened.

The high ATP-sensitivity of the $K_{ir}6.2$/SUR2A channel complex creates an inherent physiological problem: How can these channels be protective to the heart if they remain closed until catastrophic ATP depletion? Indeed, cardioprotective stimuli actually delay the opening of this channel (Brennan et al., 2015), which would be consistent with these stimuli preserving intracellular ATP levels. The presence of a second K_{ATP} channel complex with different kinetic and biophysical behaviour would be one possible solution. This idea is supported by the fact that K_{ATP} channel activators and blockers are cardioprotective and cardiotoxic, respectively, while not seemingly affecting the activity of the canonical $K_{ir}6.2$/SUR2A cardiac K_{ATP} channel complex

(Brennan et al., 2015). $K_{ir}6.1$ channels do not possess the same ATP-dependence as $K_{ir}6.2$ channels (Beech et al., 1993a, 1993b; Yamada et al., 1997; Zhang & Bolton, 1996). In vascular smooth muscle, $K_{ir}6.1$-containing channels are constitutively active at physiological levels of ATP and are instead largely regulated via phosphorylation (Hayabuchi, Dart, & Standen, 2001; Hayabuchi, Davies, & Standen, 2001; Sampson et al., 2004). In this study, we characterise the biophysical and pharmacological behaviour of a newly-identified functional $K_{ir}6.1$-like conductance at the sarcolemmal membrane in ventricular cardiomyocytes.

2 | METHODS

2.1 | Materials

Cyanide, glibenclamide, HMR1098, iodoacetic acid and pinacidil are from Merck (Gillingham, UK). PNU37883A, pioglitazone and rosiglitazone are from Biotechne Ltd (Abingdon, UK).

2.2 | Group sizes

For all experiments, the group size is provided in the corresponding figure legend. In each case, the number of animals is reported with the number of cells, where appropriate.

2.3 | Randomisation

All rats used in this study were purchased from Charles River Laboratories (UK) and housed in the animal unit at the Universities of Leicester or Liverpool. Animals were provided when they reached an appropriate size (over 250 g), and the researchers had no input into the selection of the animals. Guinea pigs and rabbits were purchased from Envigo and were supplied to the user by the animal unit with researcher having no input into the selection of animals.

2.4 | Blinding

Experiments were not blinded in this study as the experimenter was responsible on each day for the cell preparation, solution making and analysis of each completed data set. To reduce any experimental bias, or anomalous results due to errors in experiments, solutions or a difference in the cellular behaviour from an animal, all data are expressed as n = animal. Multiple experimental protocols were carried out on each day to ensure best use of each cell preparation. For whole-cell or action potential recordings, data were recorded from at least five animals in each case. For contractile function and calcium fluorescence measurements, fields of view were recorded from cells isolated from least five animals, and a mean of results of individual cells from each animal was used in all cases.

2.5 | Normalisation

Whole-cell electrophysiology recordings were normalised to cell capacitance, therefore allowing comparison of currents by normalising to cell size. Fluo-4 measurements of calcium changes were normalised to the diastolic calcium level following field stimulation (i.e., F/F_0).

2.6 | Data and statistical analysis

The data and statistical analysis comply with the recommendations of the *British Journal of Pharmacology* on experimental design and analysis in pharmacology (Curtis et al., 2022).

All statistical analysis was performed in GraphPad Prism 9 (GraphPad Software, Inc., La Jolla, CA, USA, RRID:SCR_002798); the statistical tests used for each data set are reported in each figure legend. Student's paired or unpaired *t* test and one-way or two-way ANOVA with post-test were performed as indicated in the figure legends. Post-hoc tests were run only if F achieved P<0.05 and there was no significant variance inhomogeneity. Statistics were carried out using n = animal. Significance was set at $P < 0.05$. Data are plotted as bar charts with individual mean of the day values plotted individually. Standard deviation error bars are shown. Concentration–response relationships were plotted in GraphPad Prism 9 using the following equation:

$$Y = \frac{\text{Bottom} + (\text{Top} - \text{Bottom})}{\left(1 + 10^{((\text{LogEC50} - X) * \text{HillSlope})}\right)}$$

Mean with standard deviation error bars is shown for concentration–response data.

2.7 | Validity of animal species or model selection

Adult male Wistar rats have been widely used in the literature as a source of ventricular myocytes for mechanistic and pharmacological studies of myocardial function. To further confirm our findings, we also measured the $K_{ir}6.1$ channel activity in mouse, guinea pig, rabbit and porcine cardiomyocytes.

2.8 | Ethical statement

Adult male Wistar rats and guinea pigs were killed by concussion and cervical dislocation. Rabbits were killed by an overdose of sodium pentobarbitone (Euthetal, Rhone Merieux, UK; 111 $mg \cdot kg^{-1}$ body weight, i.v.) delivered via the marginal ear vein. Mice were killed by injection with the anticoagulant heparin sodium (250 IU) and terminally anaesthetised with a combination of ketamine and xylazine. The care and schedule 1 killing of animals conformed to the requirements of the United Kingdom Animals (Scientific Procedures) Act

1986 Amendment Regulations (SI 2012/3039). Ethical approval for all experimental procedures was granted by the University of Leicester/Liverpool's Animal Welfare and Ethical Review Body (AWERB_2018_44 [Leicester] or AWC0152-AWERB [Liverpool]). Animal studies are reported in compliance with the ARRIVE guidelines (Percie du Sert et al., 2020) and with the recommendations made by the *British Journal of Pharmacology* (Lilley et al., 2020).

2.9 | Animals

Adult male Wistar rats (200–400 g) were used in this study. Wild-type and *KCNJ8*$^{-/-}$ mice were used in this study to assess the effect of genetic knock out of the *KCNJ8* subunit on the K_{ir}6.1-like conductance. Adult male Dunkin–Hartley guinea pigs (400–500 g) and male New Zealand White rabbits (0.9–1.2 kg) were used in confirmatory experiments. Porcine hearts, sourced from a local abattoir, were also used to isolate cardiomyocytes for evidence of channel activity in a species showing more similarity to human cardiac function.

2.10 | Housing and husbandry

The housing of the animals was standard and conformed to the requirements of the United Kingdom Animals (Scientific Procedures) Act 1986 Amendment Regulations (SI 2012/3039).

2.11 | Experimental procedures

No experimental procedures were carried out on animals in this study. All tissue was obtained following Schedule 1 killing.

2.12 | Sex as an experimental variable

The effect of sex and hormones on cardiovascular function is an area of ongoing research. (Blenck et al., 2016; Chicco et al., 2007). To minimise any confounding effects of the sex of the animals, this study has used only male animals.

2.13 | Detailed methods

2.13.1 | Isolation of ventricular myocytes

Adult male Wistar rats (200–400 g), or Dunkin–Hartley guinea pigs (up to 500 g), were killed by a Schedule 1 procedure of concussion and cervical dislocation. Male New Zealand White rabbits (0.9–1.2 kg) were killed with an overdose of sodium pentobarbitone (Euthetal, Rhone Merieux, UK; 111 mg·kg^{-1} body weight, i.v.) delivered via the marginal ear vein. Following Schedule 1, the heart was quickly removed from the thoracic cavity and briefly submerged into cold (4°C) Ca^{2+}-free Tyrode's solution containing (in mM): KCl 5, NaCl 135, NaH_2PO_4 0.33, Na pyruvate 5, HEPES 10, Mannitol 15, Glucose 5, $MgCl_2$ 1, EGTA 0.3, pH 7.4 (Merck), to halt contractions and to lower the metabolic demand. The isolated heart was then cannulated via the aorta and mounted on a Langendorff-type apparatus and perfused in a retrograde manner with warmed Ca^{2+}-free Tyrode's solution (37°C) for 6 min. The enzyme mix solution (19-mg collagenase; 50-mg BSA prepared from factor V albumin and 16-mg protease; type XIV 15% Ca^{2+}, Merck) was then perfused through the heart until isolated cells appeared in the perfusate sampled from the ventricles. The solution was then exchanged for Ca^{2+}-free Tyrode's solution for a further 2 min and then the heart was cut down, washed in normal Tyrode's (NT) solution containing (in mM): KCl 5, NaCl 135, NaH_2PO_4 0.33, Na pyruvate 5, HEPES 10, Mannitol 15, Glucose 5, $MgCl_2$ 1, $CaCl_2$ 2 and cardiomyocytes mechanically separated using a shaking water bath at 37°C. This technique yielded 70%–90% rod-shaped cardiomyocytes, which were stored in normal Tyrode's solution at room temperature and used within 12 h of isolation.

Freshly removed whole porcine hearts were collected from a local abattoir and transported to the laboratory in a chilled cardioplegic solution containing (in mM): 50 KH_2PO_4, 8 $MgSO_4$, 10 HEPES, 5 adenosine, 140 D-glucose, 100 mannitol, pH to 7.4 with KOH. A wedge of ventricular tissue was cut and perfused using a Langendorff apparatus with a warm Ca^{2+}-free/EGTA solution 15 min (37°C) containing (in mM): 137 NaCl, 5 KH_2PO_4, 1 $MgSO_4$, 5 HEPES, 10 D-glucose, 10 taurine, 0.2 EGTA, pH to 7.4 with KOH (Merck). The ventricular wedge was then perfused with an identical calcium free solution for 30 min, except that the EGTA was omitted. The enzyme mix solution (15-mg collagenase type II; Worthington and 50-mg BSA prepared from factor V albumin [Merck]) was then perfused through the ventricular tissue wedge until the tissue became soft, which took approximately 15 min. The wedge was then removed, and small cubes of tissue were removed and placed in Kraftbrühe (KB) solution consisting of (in mM): 90 L-glutamic acid, 30 KCl, 10 HEPES, 1 EGTA, 5 Na pyruvate, 20 taurine, 20 glucose, 5 $MgCl_2$, 5 succinic acid, 5 creatine, 2 Na_2ATP and 5 β–OH butyric acid; pH 7.4 with KOH (Merck). Cardiomyocytes were mechanically separated using a shaking water bath at 37°C in Kraftbrühe solution.

All experiments using mice were conducted in the Tinker Laboratory, Queen Mary University of London (QMUL). This work was approved by the QMUL Animal Welfare and Ethical Review Body and covered by British Home Office Project Licenses PPL/7665 and PE9055EAD. Mice were injected with the anticoagulant heparin sodium (250 IU) and anaesthetised with a combination of ketamine and xylazine. Following death, hearts were rapidly excised, cannulated on to a Langendorff apparatus and perfused with a perfusion buffer, for 4 min, containing (in mM) 113 NaCl, 4.7 KCl, 0.6 KH_2PO_4, 0.6 Na_2HPO_4, 1.2 $MgSO_4.7H_2O$, 12 $NaHCO_3$, 10 $KHCO_3$, 30 Taurine, 10 HEPES, 11 D-glucose and 10 2,3-butanedione monoxime, saturated with 95% O_2–5% CO_2 at 37°C. The hearts were perfused for 10 min with digestion buffer (perfusion buffer containing 0.9 mg·ml^{-1} collagenase [Worthington type II], 0.125 mg·ml^{-1} hyaluronidase and 12.5-μl $CaCl_2$). The ventricles were then cut into several pieces and disturbed in digestion buffer at 37°C with oxygenation for 10 min twice. The

subsequent supernatant was centrifuged for 3 min at 40 g in the presence of 5% (v/v) fetal calf serum, the cell pellet was suspended in 10 ml of perfusion buffer containing 12.5-μl $CaCl_2$ and the calcium concentration was gradually restored to 1 mM over 20 min.

The cardiomyocytes were recentrifuged for 3 min at 40 g, and the pellet resuspended in Medium 199 tissue culture medium containing the following supplements: 2 $mg \cdot ml^{-1}$ bovine serum albumin, 0.66 $mg \cdot ml^{-1}$ creatine, 0.62 $mg \cdot ml^{-1}$ taurine, 0.32 $mg \cdot ml^{-1}$ carnitine hydrochloride, 10 $U \cdot ml^{-1}$ penicillin, 10 $\mu g \cdot ml^{-1}$ streptomycin and 25-μl blebbistatin. The cardiomyocytes were seeded onto sterilised laminin-coated coverslips for 60 min in humidified incubator 5% CO_2–95% air at 37°C. Cardiomyocytes were then gently washed once with blebbistatin-free culture medium to remove unattached cells. Cells were used on the day of isolation within 9 h of cell isolation. The $K_{ir}6.1$ global KO mice used in this study have previously been described in detail including generation and genotyping (Aziz et al., 2014).

2.14 | Preparation of adenoviral constructs

Recombinant adenovirus encoding rat RNA interfering short hairpin sequences (short hairpin (sh)RNA) for knockdown of $K_{ir}6.1$ was generated using pAdEasy (Agilent Technologies, Stockport, UK) (He et al., 1998; Storey et al., 2013). Cassettes expressing shRNAs were created by ligating the following oligonucleotide into pSilencer adeno 1.0 CMV (Ambion; Thermo Fisher Scientific, Warrington, UK): 5′-ccaatgtcaggtcattcac-3′. The control shRNA sequence (Ambion) was a nontargeting shRNA with limited sequence similarity to known genes in the rat. An insert including the mutant $K_{ir}6.1$, IRES and mCherry sequences was subcloned into pENTR-1A (Invitrogen) and recombined with pAd-CMV-DEST (Invitrogen) to produce recombinant adenovirus. These cassettes included a modified cytomegalovirus promoter, shRNA insert and polyA terminator and were subcloned into the pAdTrack shuttle vector and verified by sequencing. Viral genomes were assembled by transformation of electrocompetent *Escherichia coli* BJ5183 carrying pAd-easy1 with *Pme1* linearized shuttle vector constructs. Appropriately recombined isolates were propagated in DH5α. Human embryonic kidney-293A (HEK293A, RRID:CVCL_6910) cells were used for adenoviral amplification. Once ∼90% of HEK 293A cells were lysed, the medium was aspirated and centrifuged for 5 min at 350 g. The resulting supernatant, containing the harvested adenovirus, was stored at −80°C until use.

2.15 | Culture of rat isolated cardiomyocytes

Freshly isolated cardiomyocytes were pelleted in normal Tyrode's solution and resuspended in Dulbecco's Modified Eagle's Medium (DMEM) (Thermo Fisher Scientific, Warrington, UK) with glutamax and 5-mM glucose, supplemented with 2% Pen/strep and non-essential amino acids. Five hundred microlitres of cell suspension was added to each well of a 6-well plate. Twenty to fifty microlitres of adenoviral construct was added to each well for 3 h. The media was then replaced, and the cells incubated for 48 h at 37°C and 5% CO_2 (Storey et al., 2013). For patch-clamp experiments, 200 μl of cell suspension was added directly to the glass-bottomed perfusion chamber, and the cells allowed to adhere for 10 min prior to experimentation.

2.16 | Culture of HEK283 and CHO cells

Human embryonic kidney 293 (HEK293, RRID:CVCL_0045) cells were maintained in Minimal Essential Media (MEM) with Earle's salts supplemented with 10% foetal bovine serum and 1% L-glutamine (Thermofisher; Warrington, UK)). One-percent penicillin/streptomycin solution was also added to the media and the cells maintained at 37°C in 5% CO_2. Cells were passaged using a Trypsin digest and replated in appropriate flasks or plates for transfection. $K_{ir}6.1$, $K_{ir}6.2$ or $K_{ir}6.1$--$K_{ir}6.2$ dimers were encoded in pIRES2-EGFP vectors, with the eGFP at the internal ribosome entry site. SUR2A was in a pcDNA3 vector. HEK293 cells were transfected using Lipofectamine2000™ (Thermofisher). Chinese Hamster Ovary cells (CHO, RRID:CVCL_0213) stably expressing $hK_{ir}6.1$ and hSUR2B subunits were purchased from B'SYS (Witterswil, Switzerland). CHO cells were maintained at 37°C in 5% CO_2 in F12 (HAM) medium (Merck; Thermo Fisher Scientific, Warrington, UK) supplemented with 10% fetal bovine serum, 1% penicillin/streptomycin solution, hygromycin 100 $\mu g \cdot ml^{-1}$ and puromycin 1 $\mu g \cdot ml^{-1}$ (Thermofisher) for stable selection.

2.17 | qPCR to assess *kcnj8* knockdown in CHO cells

Given a low adenoviral infection efficiency in ventricular myocytes as determined by mCherry fluorescence, the efficacy of the *kcjn8* knockdown was assessed in a CHO cell line stably expressing $K_{ir}6.1$ and SUR2B. The infection efficiency was also limited in the CHO cells, (16–20%), and so infected CHO cells underwent fluorescence-activated cell sorting (FACS) based on mCherry fluorescence using an BD FACSAria™ III cell sorter. Collected sorted cells were stored in RNA Later. Total RNA was isolated using Monarch® Total RNA Miniprep Kit (NEB), and cDNA was subsequently synthesised using LunaScript® RT SuperMix Kit (NEB) according to the manufacturer's instructions. Quantitative PCR (qPCR) reactions were performed in 20 μl using Luna® Universal qPCR Master Mix (NEB) alongside validated primers targeting *Kcnj8* (forward primer 5′-AACCTGGCGCATAAGAACATC-3′; reverse primer 5′-CCACATGATAGCGAAGAGCAG-3′) and *Gapdh* (forward primer 5′-TGTAAAGCTCATTTCCTGGTATGAC-3′; reverse primer 5′-TGTGGGGGTTATTGGACAGG-3′). Quantification was performed on an ABI ViiA-7 Thermocycler. PCR amplifications were undertaken in triplicate concurrently with no-reverse transcriptase and no-template controls. PCR cycles proceeded as follows: 95°C for 60 s (initial denaturation) then 40 cycles of 95°C for 15 s (denaturation) and 60°C for 20 s (annealing and extension) followed by a plate read. Following qPCR, the melting temperature (T_m) for each sample was ascertained via melt curve analysis. Data were exported from QuantStudio™ v1.3

(ThermoFisher, RRID:SCR_018712) and the mean threshold cycle (Ct) value for each sample was normalised to *Gapdh* using the ΔΔCt method. Statistical analyses were performed on ΔCt values.

2.18 | Generation of a $K_{ir}6.1$–$K_{ir}6.2$ fusion protein

To create a dimeric fusion protein of $K_{ir}6.1$ and $K_{ir}6.2$, silent mutations were introduced to rat $K_{ir}6.1$ cDNA and Kir6.2 cDNA in a pBFT *Xenopus laevis* oocyte expression vector to insert novel restriction sites. A *ClaI* restriction site was inserted into the 3′ end of $K_{ir}6.1$ and an *XbaI* site in the 5′ end of $K_{ir}6.2$ cDNA using a Stratagene QuikChange™ site-directed mutagenesis kit. Successful mutants were picked, and the $K_{ir}6.2$-*XbaI* mutant was subcloned into the $K_{ir}6.1$-*ClaI* mutant pBFT vector. To link the two subunits together, a *XbaI*/*ClaI* (Thermofisher) double digest was carried out and two single-stranded deoxyoligonucleotides were synthesised (University of Leicester Protein and Nucleic Acid Chemistry Laboratory [PNACL]) representing the sense and anti-sense strands to complete the ends of the $K_{ir}6.1$ and $K_{ir}6.2$ sequences with an octaglycine linker sequence between the $K_{ir}6.1$-C and $K_{ir}6.2$ N-termini. Successful fusion proteins were identified by restriction digest and sequencing. The fusion protein was then cloned into a pIRES2-EGFP mammalian expression vector and used in transient transfections in a HEK293 cell line.

2.19 | Patch-clamp electrophysiology

Patch electrodes were made from filamented thick-walled borosilicate glass with a resistance of 3–6 MΩ. Recordings were made from isolated cardiomyocytes using an Axopatch 200B amplifier, filtering at 2 kHz. Recordings were digitised using a Digidata 1440 and recorded and analysed using pCLAMP 10.3 software (Axon Instruments, Scientifica, Uckfield, UK, RRID:SCR_011323). Cells were allowed to adhere to a glass coverslip mounted in a Dagan HW-30 heated perfusion chamber (Dagan Corp, USA) for 10 min prior to experimentation. Solutions were perfused at a rate of 5 ml·min^{-1} and at 32 ± 2°C.

2.19.1 | Cell-attached

The intracellular electrode solution contained (in mM) 140 KCl, 10 HEPES, 1 $CaCl_2$ and 0.5 $MgCl_2$. In voltage-clamp mode, the electrode was held at +40 mV for the duration of the recording. Under these conditions, the equilibrium potential for potassium is close to 0 mV, and the voltage across the membrane patch is approximately −110 mV (the sum of the electrode potential and the resting potential of the cardiomyocytes, assumed to be −70 mV) so that single K_{ATP} channel openings lead to inward currents.

To investigate channel activity, the channel open probability (P_O) was calculated; however, in the majority of recordings, multiple levels of opening were observed, and so, the number of levels and duration of activity at each level was measured:

$$T_O = \sum_{L=1}^{N} t_{oL}$$

T_O represented the duration that the channel was open, where L represents different open levels, t_{oL} is the duration of time in each level and N the number of ion channels in the recording. Given that the true number of channels cannot be measured because of the stochastic behaviour of ion channels, the number of channels is taken as the maximum number of levels open during the total (T) duration of the recording. The open probability was presented as NP_O:

$$NP_O = \frac{T_O}{T}$$

To produce current–voltage relationships, the amplitude of the openings was measured at voltages ranging from −180 to 10 mV. Sampling rate for cell attached recordings was 50 kHz (Brennan et al., 2015, 2019; Sims et al., 2014). Data were analysed in pCLAMP10 using a threshold set to 4.5 pA per open channel level. This allowed the 30-pS $K_{ir}2.x$ current to be largely filtered out as a change in baseline, given its long open durations, compared with the larger (40-pS), bursting $K_{ir}6.1$-like channel. For experiments to measure glibenclamide concentration–response data, glibenclamide was included in the patch pipette in cells tested and compared with control cells (no glibenclamide in the pipette). Given the variability of the NP_O, the geometric mean of the day was calculated for each data point presented in the cell attached configuration. Data are, therefore, reported as n = animals. Sixty seconds of data was used to measure the NP_O for each cell. Data are expressed as paired (where control recordings at the end of 3 min of recording are then compared to the end of 4 min of perfusion with the drug) or unpaired (when separate recordings are made on the day for control and drug-treated cells). For unpaired data, at least five control and five drug-treatment cells were recorded for each animal for a mean of the day data point. For channel kinetics, open dwell and closed times analysed from cell attached recordings. Data were resampled at 25Khz, idealised in QuB (Quantify Unknown Biophysics, https://qub.mandelics.com/) (QuB with K-segmental means as described previously (Davies et al., 2010; Qin, 2004). In all cases, a single cell attached recording was made from a cell.

2.19.2 | Excised-patch recording

$K_{ir}6.1$, $K_{ir}6.2$ or $K_{ir}6.1$–$K_{ir}6.2$ dimer constructs were transiently transfected into HEK293 cells using Lipofectamine™2000 reagent (Invitrogen), with the eGFP fluorescent protein expression used in the identification of transfected cells. Experiments were carried out using excised inside-out patch recording, where solutions were perfused directly on to the inside face of the patch using a gravity-fed perfusion system. Patches were held at E_K (approximately 0 mV) and currents recorded by pulsing to the equivalent of −80 mV 20 times for 100 ms for each pulse. The mean of the last 20 ms for each pulse was

averaged to give a single mean current value for each concentration of ATP and bathing solution in the absence of ATP.

2.19.3 | Whole-cell

Intracellular electrode solution contained (in mM) 30 KOH, 110 KCl, 10 EGTA, 10 HEPES, 1 $MgCl_2$, 1 Mg-ATP, 0.1 Na-ADP, 0.1 GTP and 20 nM $CaCl_2$, pH 7.2 with HCl.

Action potential (AP)

In current-clamp mode, APs were stimulated at 1 Hz via the patch electrode with a 5-ms depolarizing trigger, set to 130% of that required to elicit an AP (approximately 500–900 pA). Action potential duration to 90% repolarized (APD_{90}) and membrane potential (V_m) were calculated within pCLAMP software offline (Brennan et al., 2015, 2019; Sims et al., 2014).

Whole-cell currents

In voltage-clamp mode, the membrane potential was held at 0 mV to inactivate most voltage-gated current. Pharmacological modulation of K_{ATP} channels was used to look at these whole-cell currents in isolation, with glibenclamide at 10 μM being used to define no K_{ATP} current. A second protocol using a voltage-step from −70 to −20 mV to investigate the potential $K_{ir}6.1$ component of the IK_1 current was used.

2.20 | Video edge detection measurements of contraction

Cells were allowed to adhere to a glass coverslip mounted in a Dagan HW-30 heated perfusion chamber (Dagan Corp, USA) for 10 min prior to experimentation. Solutions were perfused at a rate of 5 $ml{\cdot}min^{-1}$ and at 32 ± 2°C. Cardiomyocytes were stimulated to contract using electric field stimulation (EFS) at 1 Hz. Contractile function was observed via a JVC CCTV camera and recorded to DVD for offline analysis. Video edge detection was carried out a video edge detection system (Crescent Electronics), digitised using a Minidigi 1B interface (Axon instruments) and recorded using Axoscope 10.7 software (Axon instruments, RRID:SCR_011323). Arbitrary measurement units were calibrated, using an eyepiece graticule, to μm.

2.21 | Fluo-4 measurements of intracellular calcium transients

Isolated cardiomyocytes were incubated with 5 $\mu mol{\cdot}L^{-1}$ Fluo-4-AM (Thermofisher) indicator at room temperature for 30 min. Cells were allowed to adhere to a glass coverslip mounted in a Dagan HW-30 heated perfusion chamber (Dagan Corp, USA) for 10 min prior to experimentation. Solutions were perfused at a rate of 5 $ml{\cdot}min^{-1}$ and at 32 ± 2°C. Cardiomyocytes were stimulated to contract using electric field stimulation (EFS) at 1 Hz. Fluo-4 fluorescence was excited at 480 nm excitation light from a PTI-monochromator with emissions collected above 520 nm using an Andor Zyla 4.5 Camera with images recorded to Winfluor software (John Dempster, University of Strathclyde). To record the Ca^{2+} transients, images were acquired at a rate of 40 frames s^{-1} and 2 × 2 pixel binning was used to improve the signal-to-noise ratio given the short exposure time (25 ms).

2.22 | Computer simulations

Action potentials were simulated in the OpenCOR 0.7.1 (RRID:SCR_019001) environment using an established 'Rudy-O'Hara-CiPA version' ventricular cardiomyocyte model (Chang et al., 2017; Dutta et al., 2017; Li, Dutta, et al., 2017; O'Hara et al., 2011). The original model is available at https://models.cellml.org/e/5a0/ohara_rudy_cipa_v1_2017.cellml/view.

To simulate the effects of the K_{ATP} channels to the action potential duration, we modified the model to include both K_{ATP} channel isoforms.

The equation used to describe the $K_{ir}6.2$ channel (IKatp62) was

$$IKatp62 = GKatp62 * dATPi62 * dHMR62 * (V - EK)$$

where IKatp62 is the whole-cell current produced via $K_{ir}6.2$ channels. V is membrane potential, E_K is the equilibrium potential for K^+ and GKatp62 is the $K_{ir}6.2$ membrane conductance. The value of GKatp62 was estimated from the maximum current observed in the presence of a metabolic inhibitor (i.e., with ATP depletion meaning minimal ATP block of the $K_{ir}6.2$ channel). Rat cardiomyocytes held at 0 mV, with an E_K of −87 mV, have a metabolic-inhibition activated current of 9405 pA. This gives a conductance value of 720-$pS{\cdot}pF^{-1}$, assuming a cell capacitance of 150 pF.

dATPi62 and dHMR62 describe the fraction of open channels based on ATP inhibition and HMR1098 block, respectively; both were described by Hill equations.

$$dATPi62 = \frac{1}{1 + \left(\frac{ATPi}{IC50_{ATP}}\right)^{Hill}}$$

where ATPi is the internal concentration of ATP, $IC50_{ATP}$ is the intracellular concentration of ATP that inhibits the channel by 50% and Hill is the Hill slope of the concentration–response curve. IC_{50} values for ATP-induced inhibition (21.9 μM for $K_{ir}6.2$/SUR2A expressed in HEK293 cells) from Figure S3.

To simulate how ATPi block is altered by 50 or 200 μM pinacidil, the IC_{50} value was right-shifted, based on published experimental data showing the mechanisms of K_{ATP} channel activation by pinacidil (Fan et al., 1990).

dHMR62 describes the open probability of the channel, based on HMR1098 block on $K_{ir}6.2$/SUR2A expressed in HEK293 cells (Rainbow et al., 2005).

$$dHMR62 = 1 - \left(\frac{1}{1 + \left(\frac{HMR}{IC50_{HMR}} \right)^{Hill}} \right)$$

The equation used to describe the $K_{ir}6.1$ channel was

$$IKatp61 = GKatp * dPNU61 * dPIN61 * (V - EK)$$

where IKatp61 is the whole-cell current produced via $K_{ir}6.1$ channels. V is membrane potential, E_K is the equilibrium potential for K^+ and GKatp61 is the $K_{ir}6.1$ membrane conductance. The value of GKatp61 was calculated from the whole-cell PNU37883A-sensitive current in rat ventricular cardiomyocytes reported in Figure 4. Cardiomyocytes held at 0 mV, with an E_K of −87, had a PNU-sensitive current of 75 pA. Assuming a cell capacitance of 150 pF gives a GKatp61 value of 5.7-pS·pF^{-1}. dPNU61 and dPIN61 describe how the fraction of open channels is altered by the presence of PNU or pinacidil using the Hill equation.

$$dPNU61 = 1 - \left(\frac{1}{1 + \left(\frac{PNU}{IC50_{PNU}} \right)^{Hill}} \right)$$

where PNU is the concentration of PNU, $IC50_{PNU}$ is the concentration of PNU to inhibit the response by 50% and Hill is the Hill slope on the concentration–response curve. The values of $IC50_{PNU}$ and Hill were based on the whole-cell PNU37883A concentration–response curve recorded in CHO $K_{ir}6.1$/SUR2B cells (Figure S5).

$$dPIN61 = 1 + \left(\frac{1}{1 + \left(\frac{EC50_{PIN}}{PIN61} \right)^{Hill}} \right)$$

$EC50_{PIN}$ is the concentration of pinacidil that increased the response by 50%, PIN61 is the test concentration of pinacidil and Hill is the Hill slope on the concentration–response curve. The EC_{50} and Hill slope values used in in the model were from the whole-cell pinacidil concentration–response curve using CHO Kir6.1/SUR2B cells (Figure S5).

Finally, IKB current, a background leak K^+ current in the model which had similar voltage-profile to $K_{ir}6.1$, was reduced to compensate for the addition of the drug-sensitive $K_{ir}6.1$ channel. A one-third deduction of the IKB conductance in the model allowed the accommodation of the K_{ATP} channels with little effect to the overall shape to the action potential waveform. Model validation is shown in Figure S8.

2.23 | Nomenclature of targets and ligands

Key protein targets and ligands in this article are hyperlinked to corresponding entries in the IUPHAR/BPS Guide to PHARMACOLOGY http://www.guidetopharmacology.org and are permanently archived in the Concise Guide to PHARMACOLOGY 2023/23 (Alexander, Fabbro et al., 2023; Alexander, Mathie et al., 2023).

3 | RESULTS

3.1 | A 40-pS channel, with a $K_{ir}6.1$-like biophysical fingerprint, is constitutively active at the ventricular cardiomyocyte surface membrane

In cell-attached patch recordings from Wistar rat ventricular myocytes, metabolic inhibition activated the canonical $K_{ir}6.2$/SUR2A K_{ATP} complex, with a conductance of 79-pS as described previously (Figure 1a) (Aguilar-Bryan et al., 1998; Brennan et al., 2015, 2019; Inagaki, Gonoi, et al., 1995; Inagaki, Tsuura, et al., 1995; Noma, 1983). $K_{ir}6.2$/SUR2A is inhibited by normal physiological ATP concentrations of up to ∼6 mM (Tran et al., 2015) and only activates when intracellular ATP is reduced below 100 μM (IC_{50} for ATP 20–30 μM; Brennan et al., 2020; Rainbow, James, et al., 2004; Rainbow, Lodwick, et al., 2004). Prior to this metabolic inhibition-induced activation, there was an additional ∼40-pS channel that displayed bursting behaviour similar to $K_{ir}6.1$-containing channels (Figures 1a[ii] and S1). Importantly, this constitutively active channel was distinct from the $K_{ir}2.x$ inwardly rectifying current, which displayed characteristic openings of long duration and had a conductance of ∼30-pS (Figures 1b,c and S2). This 40-pS constitutively active channel had a reversal potential of 0 mV in the symmetrical K^+ recording conditions and displayed weakly rectifying voltage-independent inward current properties. These data suggest a weak inwardly rectifying K^+ channel but was again distinguished from the $K_{ir}2.x$ strong inwardly rectifying current, which had a smaller conductance (30-pS) and no discernible openings positive to E_K (Figure 1c). The kinetics of the 40-pS channel in terms of open and closed dwell times were similar to those reported previously for heterologously expressed $K_{ir}6.1$/SUR2B channels (Davies et al., 2010) (Figure 1d,e).

The single channel conductance of the constitutively active 40-pS channel was compared to K_{ATP} channel subunits heterologously expressed in HEK cells. It was found to be near identical to that of $K_{ir}6.1$ channels transiently coexpressed with SUR2A (38-pS; Figure S3) and comparable to conductance values previously reported for $K_{ir}6.1$ channels with SUR2A or 2B (33–52-pS; Aziz et al., 2018; Han et al., 1996; Takano et al., 1998; Yamada et al., 1997). Similarly, the single-channel conductance and kinetic behaviour of the larger and late-activating metabolically sensitive cardiomyocyte channel was comparable to that of Kir6.2 channel monomers co-expressed with SUR2A in HEK cells (Figure S3). K_{ATP} channels have also been reported to form dimers of $K_{ir}6.1$/$K_{ir}6.2$ in heterologous expression systems with a conductance intermediate between $K_{ir}6.1$ and $K_{ir}6.2$ homomers (Cui et al., 2001; Kono et al., 2000). This is unlikely to be the case in the cardiomyocytes as the conductance of the newly identified channel did not match the conductance of channels formed from $K_{ir}6.1$–$K_{ir}6.2$ dimers expressed in HEK293 cells (Figure S3) and previous reports show $K_{ir}6.1$ and $K_{ir}6.2$ do not heteromultimerize in cardiac myocytes (Seharaseyon et al., 2000). In addition, $K_{ir}6.1$–$K_{ir}6.2$ dimers retain sensitivity to ATP-dependent block with IC_{50} values identical to $K_{ir}6.2$ (Figure S3), which would render such channels closed under normal physiological conditions in cardiomyocytes. Finally, this 40-pS channel was identified in cardiomyocytes isolated from several other species (Figure S4).

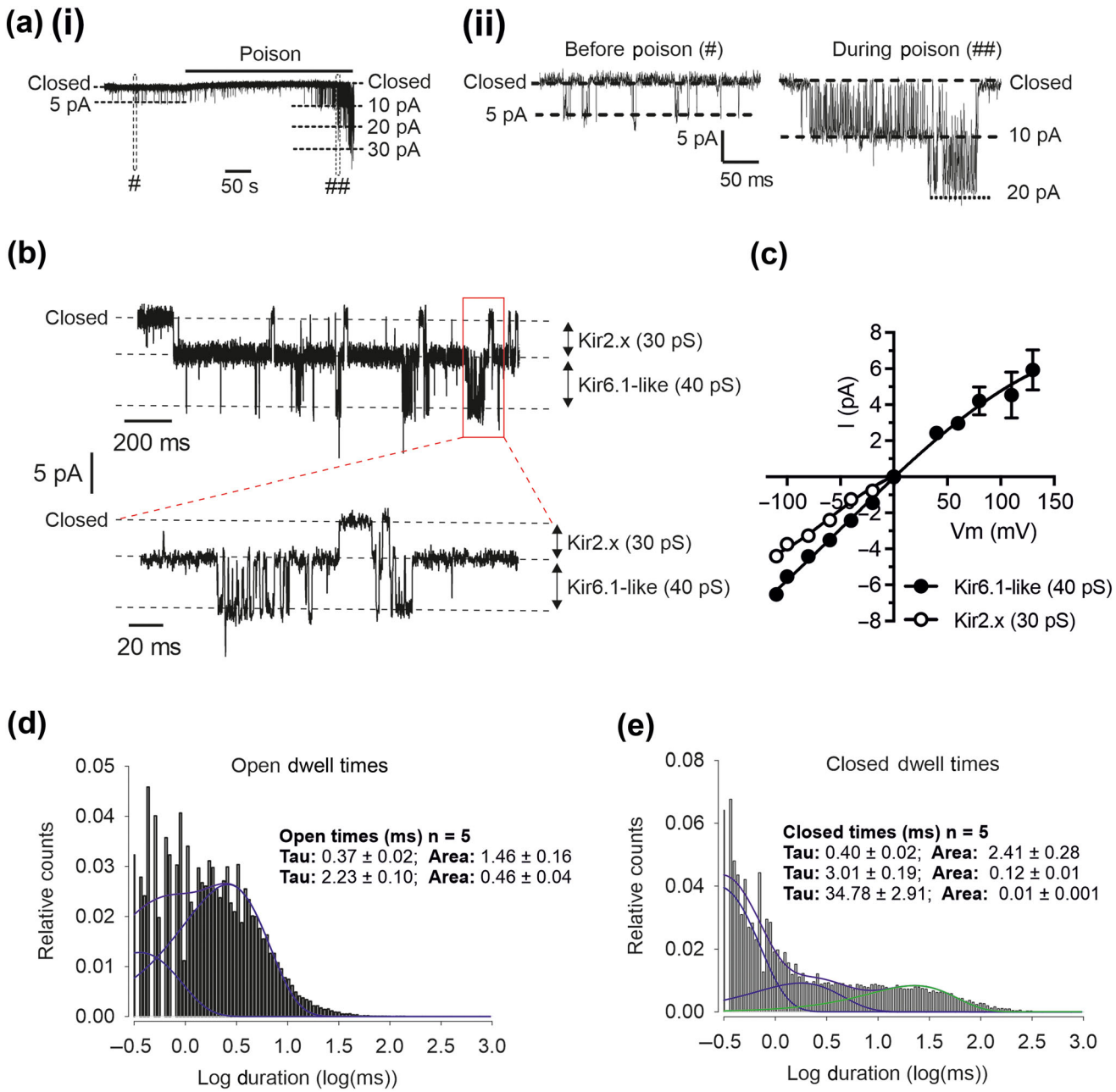

FIGURE 1 Identification of a constitutively active sarcolemmal K^+ channel in rat ventricular cardiomyocytes: (a) Constitutively active 40-pS K^+ channel openings observed (i) before the metabolic poison (2-mM cyanide and 1-mM iodoacetic acid in substrate-free Tyrode's solution) activates classic cardiac 79-pS $K_{ir}6.2$ channel activity in cell-attached patch recording. Patch electrode was held at +40 mV with an approximate membrane difference of −110 mV. (ii) Representative traces of cell-attached patch experiment from a rat cardiomyocyte displaying smaller K^+ channel before (#) metabolic poison and $K_{ir}6.2$ channels after poison (##). (b) Example traces from cell-attached patch experiment showing $K_{ir}2.x$ channels (top) and the newly identified 40-pS channel (bottom). (c) Mean single channel IV from six cardiomyocytes showing Kir2.x strongly rectifying (30-pS) inward current up to 0 mV, but not seen in the outward direction. Putative $K_{ir}6.1$ weakly rectifying (40-pS) channels were seen across the voltage range tested. Representative examples of open dwell (d) and closed (e) times; mean data analysed from five cell attached recordings. Data were re-sampled at 25 kHz, idealised in QuB (Quantify Unknown Biophysics, https://qub.mandelics.com/) with K-segmental means as described previously (Davies et al., 2010; Qin, 2004). Similarly, Davies et al. showed two distinct open and three distinct closed states suggesting similar channel biophysical characteristics in the HEK293 cell model compared with the data in cardiomyocytes presented here.

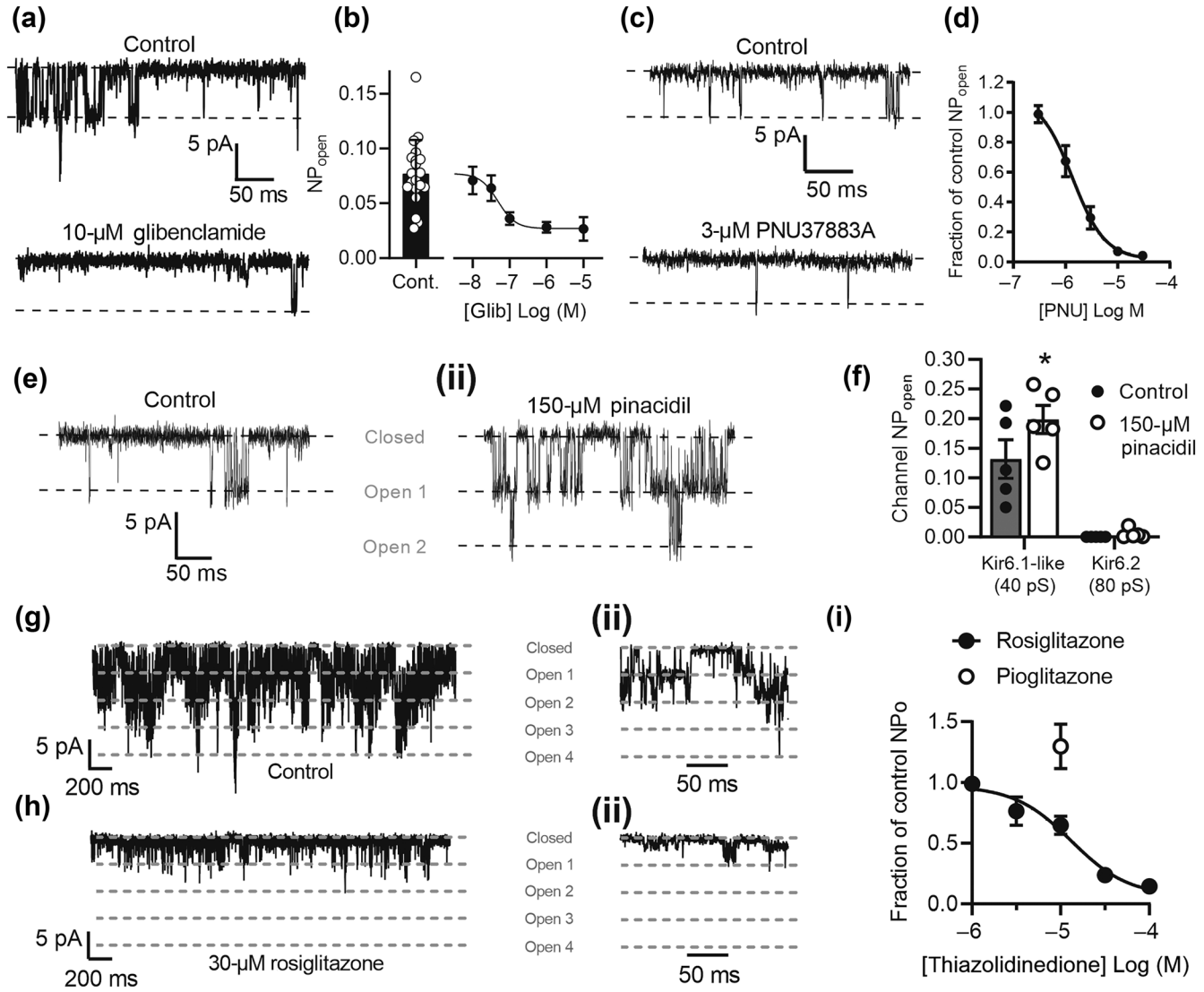

FIGURE 2 Pharmacological modulators of K_{ATP} channels alter the activity of the $K_{ir}6.1$-like 40-pS channel in cell-attached patch recording. (a) Representative recordings of the $K_{ir}6.1$-like 40-pS channel openings in the absence and presence of the pan-K_{ATP} channel blocker glibenclamide (10 μmol·L^{-1}). (b) Concentration–response curve showing the K_{ATP}-like channel NP_O in the presence of glibenclamide (IC_{50} of 47 ± 4 nM, each data point n = ≥ 5 animals, n = 26 animals in total [236 cells]). (c) Representative recordings of the $K_{ir}6.1$-like 40-pS channel with the selective $K_{ir}6.1$ blocker PNU37883A (PNU)(3 μmol·L^{-1}). (d) Concentration–response curve showing NP_O in the presence of PNU (IC_{50} of 1.5 ± 0.2 μM, n = 9 animals). (e) Example trace of $K_{ir}6.1$-like channel (i) in control conditions and (ii) in perfusion with 150 μmol·L^{-1} pinacidil. (f) Bar chart showing that 150 μmol·L^{-1} pinacidil increased the NP_O of the smaller, $K_{ir}6.1$-like channel, and caused little change in $K_{ir}6.2$ channel activity (* P<0.05, two-way ANOVA with Sidak's multiple comparisons test, n = 5 animals). (g) Example of cell-attached patch recording (i) in control conditions, (ii) same with an expanded section and (h) showing decreasing $K_{ir}6.1$ activity (i) with 30 μM rosiglitazone, (ii) same with an expanded example trace. (i) Concentration–response data to rosiglitazone showing a reduction in NP_O with increasing concentration of drug (IC_{50} = 13.5 ± 0.5 μM, n = ≥ 5 animals for each data point, eight animals in total [27 cells]). Pioglitazone had no inhibitory effect on Kir6.1 NP_O (n = 6 animals).

3.2 | The 40-pS channel has pharmacological properties that match the $K_{ir}6.1$ channel

To determine whether this newly identified Kir6.1-like channel displayed similar pharmacology to a K_{ATP} channel, established K_{ATP} modulators were used. The open probability (NP_O) of the constitutively active 40-pS channel was reduced by the pan-K_{ATP} channel blocker **glibenclamide** (10 μM; Figure 2a,b) and had an IC_{50} of 47 ± 4 nM. This compares with an IC_{50} of 40 ± 10 nM for whole-cell recording of $hK_{ir}6.1$/hSUR2B stably expressed in CHO cells (Figure S5). The selective $K_{ir}6.1$ pore-blocker **PNU37883A** (PNU) (Cui et al., 2003; Kovalev et al., 2004; Teramoto, 2006), also significantly reduced the NP_O of the constitutively active channel (Figure 2c,d). PNU has been reported to partially (40%) block $K_{ir}6.2$/SUR2A channels at very high concentrations (>10 μM) (Cui et al., 2003), but here, PNU blocked the constitutively active channel with an IC_{50} of 1.5 ± 0.2 μM (Figure 2d). In

whole-cell recording of hK$_{ir}$6.1/hSUR2B stably expressed in CHO cells, we recorded a similar IC$_{50}$ of 1.5 ± 0.8 μM (Figure S5). In addition to inhibitors, treatment with 150 μM **pinacidil** gave a significant increase in the 40-pS channel activity but did not give a significant increase in the activation of the canonical K$_{ir}$6.2/SUR2A complex (Figure 2e,f). In whole-cell recording of hK$_{ir}$6.1/hSUR2B stably expressed in CHO cells, we recorded an EC$_{50}$ for pinacidil of 1.8 ± 0.6 μM (Figure S5). In further pharmacological evidence for K$_{ir}$6.1 channel activity, **rosiglitazone**, a thiazolidinedione compound with a reported off-target effect of blocking K$_{ir}$6.1 (Yu et al., 2011, 2012), inhibited the newly identified channel with an IC$_{50}$ of 14.5 ± 0.5 μM, whereas the related compound, **pioglitazone**, had no effect, as previously demonstrated by Yu et al (Figure 2g–i). In whole-cell recording of hKir6.1/SUR2B in CHO cells, rosiglitazone was able to inhibit pinacidil-activated current

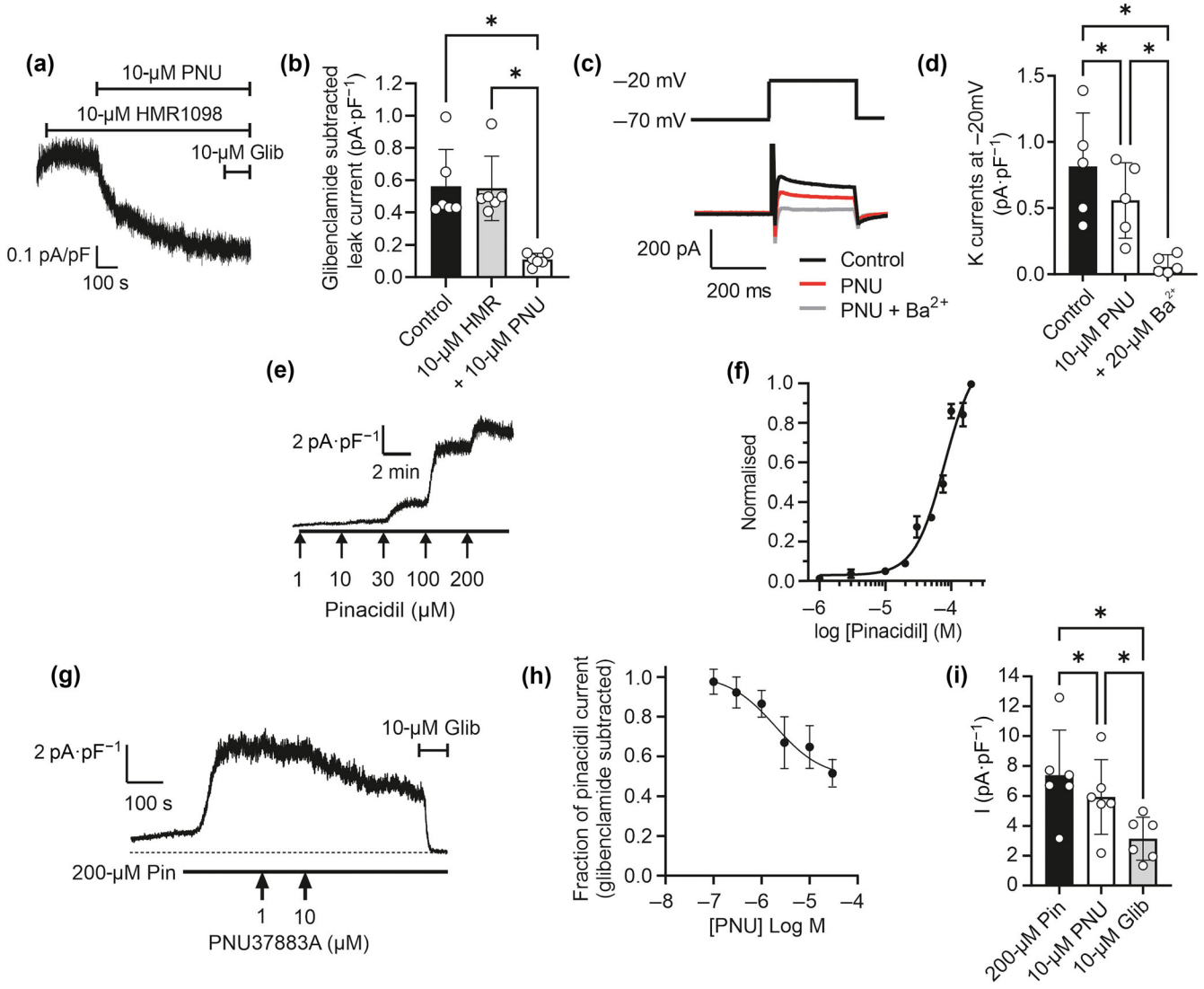

FIGURE 3 Rat ventricular myocyte glibenclamide-sensitive current, including that activated by pinacidil, has two components indicative of distinct K$_{ir}$6.1 and K$_{ir}$6.2 channels. (a) Representative trace of background current recorded in the presence of selective K$_{ir}$6.2 blocker HMR1098 (HMR) (10 μM), HMR plus selective K$_{ir}$6.1 blocker PNU37883A (PNU) (10 μM) and plus pan-K$_{ATP}$ blocker glibenclamide (10 μM). Mean data in (b) (*P<0.05, repeated measures ANOVA with Tukey's post-test, n = 6 animals [10 cells]). (c) Example trace from a whole recording from an isolated cardiomyocyte at −20 mV in control conditions and the presence of 10 μM PNU and with 20 μM Ba^{2+}. (d) Bar chart showing mean inhibition of current simulated by a depolarising pulse to −20 mV in the presence of PNU and with Ba^{2+} (*P<0.05, repeated-measures ANOVA with Tukey's post-test, n = 5 animals [8 cells]). (e) Example trace of whole-cell recording with increasing concentration of pinacidil and (f) corresponding concentration response profile from nine cells. (g) Example recording from a rat ventricular myocyte showing pinacidil activated current at 0 mV partially inhibited by PNU37883A and fully inhibited by 10 μM glibenclamide. (h) Concentration–inhibition curve of the glibenclamide-sensitive pinacidil-induced current by PNU37883A. IC$_{50}$ for the PNU37883A-sensitive component was 1.9 ± 0.3 μM (n = ≥ 5 animal for each data point, 23 animals in total (39 cells). (i) Mean current normalised to cell capacitance in the presence of pinacidil, PNU37883A and glibenclamide showing a significant reduction in current with PNU37883A and glibenclamide (*P<0.05, repeated-measures one-way ANOVA with Tukey's post-test, n = 6 [control], 6 [10 μM PNU37883A] and 6 [glibenclamide]).

with an $IC_{50} = 22.6 \pm 1.7$ μM (Figure S5). As with the cell-attached patch data, pioglitazone did not show any inhibition of whole-cell current in CHO cells (Figure S5).

Consistent with the idea that canonical $K_{ir}6.2$/SUR2A channels are inactive at rest while the newly identified channel is open, the selective $K_{ir}6.2$ blocker, **HMR1098** (Manning Fox et al., 2002; Rainbow et al., 2005), had no effect on the whole-cell background currents in cardiomyocytes, whereas application of PNU (a $K_{ir}6.1$ channel pore blocker) reduced resting currents at 0 mV (Figure 3a,b). HMR1098 (a selective $K_{ir}6.2$/SUR2A blocker) was effective at reversing around 70% of the 200 μM pinacidil-induced current. Addition of PNU (a $K_{ir}6.1$ pore blocker) was able to reverse the remaining glibenclamide-sensitive current (Figure S6A,B).

Given the weakly rectifying properties, and constitutive activity, of $K_{ir}6.1$ channels, it was hypothesised that the sum of activity of $K_{ir}6.1$ and $K_{ir}2.x$ channels would contribute to the IK_1 current in cardiomyocytes. To assess the putative contributions of $K_{ir}6.1$ and $K_{ir}2.x$ channels underlying the IK_1 current, 200 μM Ba^{2+} was used, a concentration known to block inward rectifier currents (Quayle et al., 1993). At −20 mV, PNU was able to inhibit around 25% of

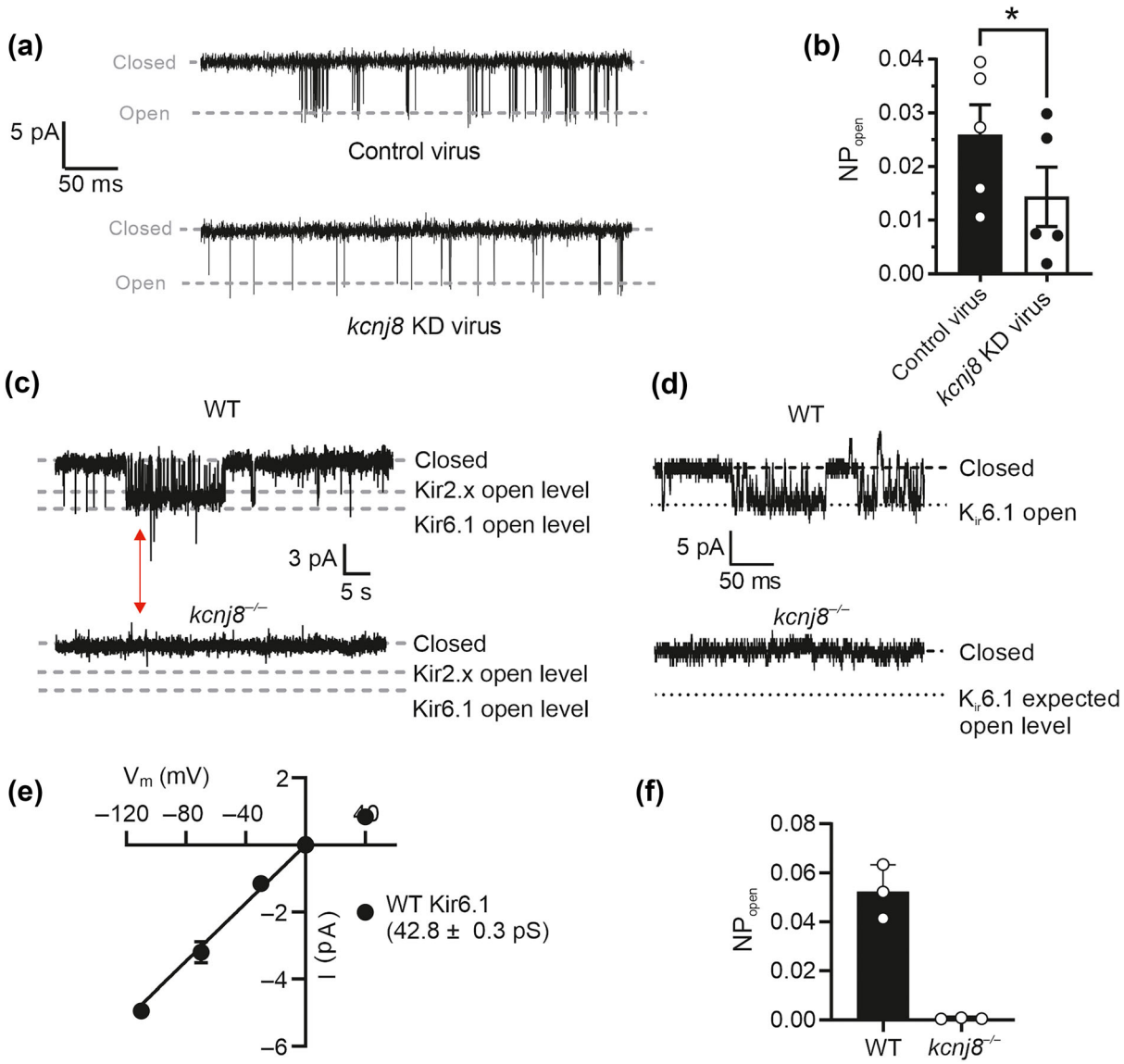

FIGURE 4 Genetic manipulation of *kcnj8* alters the constitutive activity of the proposed $K_{ir}6.1$ channel. (a) Example traces of cell attached recording from rat cardiomyocytes cultured for 48 h following a 3-h infection with adenovirus containing a control shRNA (top)or *kcnj8*-targeting knockdown (bottom). (b) Mean NP_O for the control and *kcnj8*-KD virus from five animals (*P<0.05, unpaired *t* test, 36 and 42 cells for control virus and *kcnj8*-knockdown, respectively). Each data point represents the geometric mean of the day. (c) Example traces from WT (top) and *kcnj8*$^{-/-}$ mouse-derived (bottom) cardiomyocytes. (d) Expanded example traces showing the opening of $K_{ir}6.1$ channels in the WT trace (top), but not in the *kcnj8*$^{-/-}$ mouse-derived cardiomyocytes (bottom). Red arrow in (c) shows where the expanded traces were taken from (e) mean current–voltage relationship from WT animals for the putative $K_{ir}6.1$ channel (n = 3 animals). (f) Mean NP_O expressed by animal showing no discernible activity of the putative $K_{ir}6.1$ channel in *kcnj8*$^{-/-}$ animals (n = 3 animals for both WT [17 cells] and *kcnj8*$^{-/-}$ [19 cells]).

the current, with up to 90% of the remaining current being sensitive to Ba^{2+} ion block (Figure 3c,d). These data, together with the single channel current–voltage relationship (Figure 1b,c), further support the hypothesis that this newly identified current is distinct from $K_{ir}2.x$ channels.

With perfusion of increasing concentrations of pinacidil, whole-cell pinacidil-activated currents were detectable between 1 and 30 μM, with a larger increase in current at concentrations >100 μM (Figure 3e,f). These data are consistent with the hypothesis that there are two K_{ATP} complexes in cardiac cells. In vascular smooth muscle cells, which express K_{ATP} channels made up of $K_{ir}6.1$/SUR2B subunits, the application of 10 μM pinacidil is sufficient to give a substantial increase in the K_{ATP} current. In contrast, in cardiac cells, where the canonical complex is $K_{ir}6.2$/SUR2A, 100 to 200 μM pinacidil is required to evoke a substantive response (Brennan et al., 2020; Lodwick et al., 2014; Rainbow et al., 2005, 2006). In a CHO cell line stably expressing human $K_{ir}6.1$/SUR2B, maximal whole-cell current was activated by 10 μM pinacidil with an EC_{50} concentration of ~1 μM (Figure S5A), which was substantially lower than that reported for $K_{ir}6.2$/SUR2A (38 μM) (Lodwick et al., 2014). In the presence of 200 μM pinacidil, to fully activate both the putative $K_{ir}6.1$ and $K_{ir}6.2$ components of I_{KATP}, there was a PNU-sensitive component that accounted for ~30% of the total K_{ATP} current. Glibenclamide was added at the end of each recording to establish a baseline of no K_{ATP} channel activity in the cardiomyocyte, and so all data are expressed as glibenclamide-sensitive current. This PNU-sensitive component had an IC_{50} of 1.6 ± 0.3 μM (Figure 3g–i), consistent with it being a $K_{ir}6.1$-pore block. Addition of 10 μM HMR1098 to inhibit the $K_{ir}6.2$/SUR2A current, following perfusion with 10 μM PNU, abolished the remaining glibenclamide-sensitive current (Figure S6C,D). These data were also consistent with the findings of the efficacy of PNU in a CHO cell line stably expressing $K_{ir}6.1$/SUR2B, where the whole-cell pinacidil-activated current was inhibited with an IC_{50} of 1.5 ± 0.8 μM (Figure S5B).

3.3 | Manipulation of KCNJ8 expression changes the putative $K_{ir}6.1$ channel activity

To further investigate whether the 40-pS channel was indeed a channel formed of Kir6.1 subunits, an adenoviral shRNA construct was introduced to the ventricular myocytes to knockdown $K_{ir}6.1$ (*KCNJ8*-KD), an approach used previously in rat ventricular myocytes for $K_{ir}6.2$ (Storey et al., 2013). In cell-attached patch recording, the 40-pS current was significantly reduced following 48-h infection with *KCNJ8*-KD virus compared to a control virus (Figure 4a,b). This *KCNJ8*-KD virus was also able to reduce the current in CHO cells stably expressing $hK_{ir}6.1$/hSUR2B with knockdown confirmed by qPCR (Figure S7). Finally, in a $KCNJ8^{-/-}$ knockout mouse model, there were no openings consistent with a $K_{ir}6.1$-like channel in the knockout animals, however this was present in the WT animals (Figure 4c–f).

The data presented in Figures 1–4 suggests on the basis of (1) biophysical characteristics (channel conductance, kinetics and rectification), (2) response to pharmacological reagents, (3) constitutive activity and (4) shRNA knockdown, that the newly-identified 40-pS channel is formed from $K_{ir}6.1$ subunits. Importantly, this channel is distinct from the Kir2 family members also expressed in ventricular cardiomyocytes.

3.4 | Direct $K_{ir}6.1$ inhibition prolongs ventricular action potential duration, increases calcium accumulation and increases contractile amplitude

The $K_{ir}6$ family shows weak inward rectification (demonstrated in Figures 1b,c and S3B) and is therefore active across the voltage range experienced by cardiomyocytes during the cardiac excitation cycle. Given the constitutive activity of the $K_{ir}6.1$-like channel recorded across the range of membrane potentials, we hypothesised that inhibition of this channel would prolong the cardiac action potential duration (APD) and alter Ca^{2+} transient amplitude and duration. To assess this, rat cardiomyocyte APD was measured in the presence and absence of $K_{ir}6.1$ blocker PNU (3 μM) and pan-K_{ATP} channel blocker glibenclamide (10 μM). The APD_{90} was prolonged by 20–30 ms in the presence of either PNU or glibenclamide (Figure 5a,b). Neither drug altered the resting membrane potential, which is likely due to the small driving force at resting potentials for K^+ currents. Additionally, shRNA-*KCNJ8* knockdown caused a prolongation of the action potential in rat ventricular myocytes (Figure 5b). These data are consistent with computer simulations of the ventricular AP, where partial block of the $K_{ir}6.1$ current, by modelling the effects PNU on the open probability of the channel, prolonged the duration of the simulated AP (Figure 5c), consistent with the prolongation seen in rat cardiomyocytes (Figure 5a). Furthermore, complete removal of the model's $K_{ir}6.2$ current under physiological conditions did not alter APD (Figure S8). Consistent with its high ATP-sensitivity, $K_{ir}6.2$ only shortened APD when intracellular ATP was reduced as previously shown both experimentally (Nakayama et al., 1990) and in computer simulations (Matsuoka et al., 2003). PNU (3 μM) also increased $[Ca^{2+}]_i$ in cardiomyocytes during the calcium transients as measured by the area under the curve and peak Fluo-4 signal (Figure 5d,e), which resulted in larger myocyte contractions when measured using video edge detection (Figure 5f,g). These data suggest that the constitutive activity of these $K_{ir}6.1$-containing channels influences APD and thus the amount of Ca^{2+} entering the cell during the cardiac excitation cycle.

3.5 | $K_{ir}6.1$ potentiation by pinacidil shortens the action potential duration, reduces calcium accumulation during each contractile cycle and reduces the amplitude of contraction

Having demonstrated that pharmacological inhibition and $K_{ir}6.1$ subunit knockdown can prolong the APD (Figure 5), we hypothesised that activation of the $K_{ir}6.1$ channel would cause AP shortening. To test this, pinacidil (150 μM) was used to potentiate $K_{ir}6.1$ since this concentration had no effect on $K_{ir}6.2$ activity in cell attached recordings

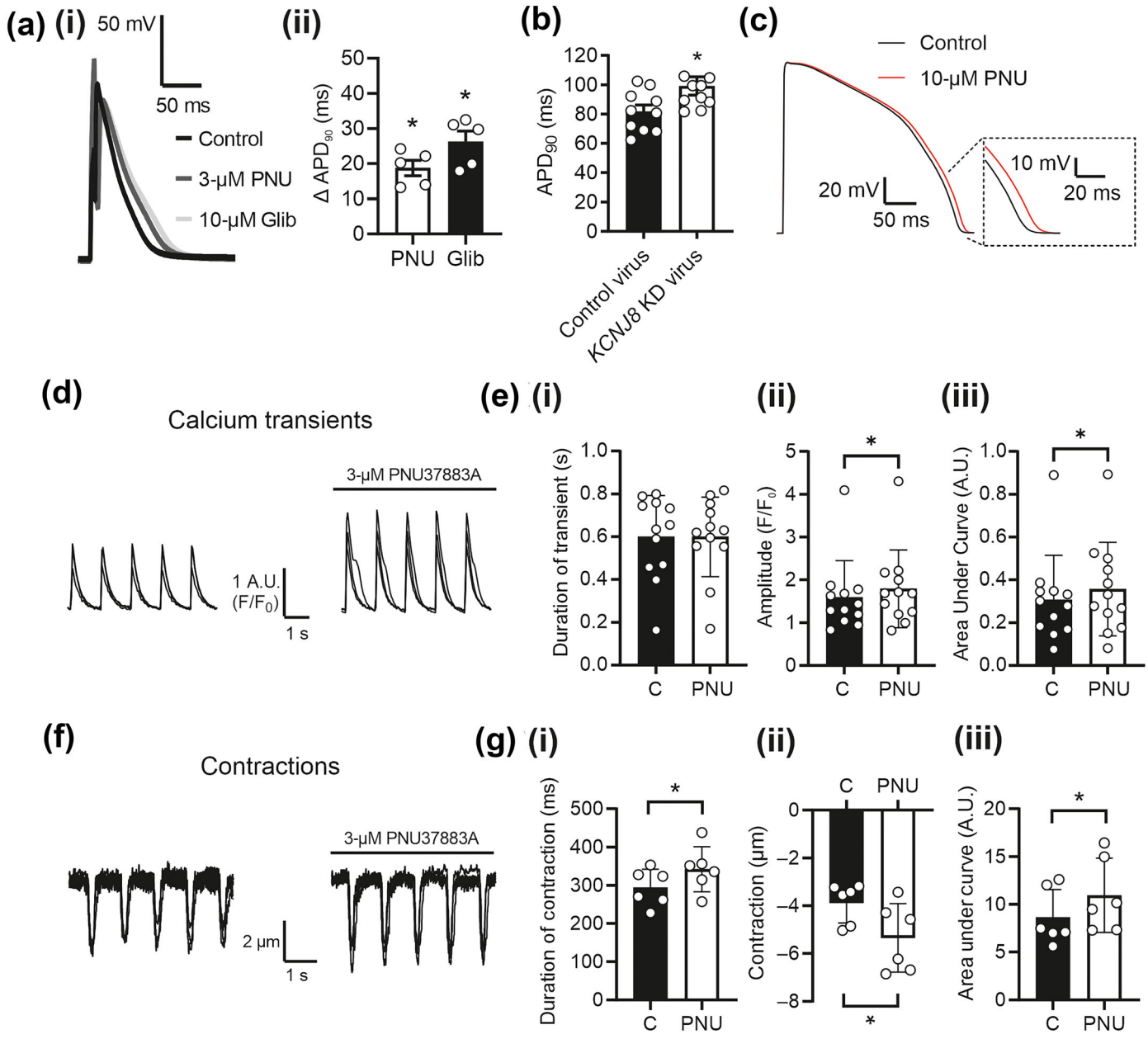

FIGURE 5 Direct $K_{ir}6.1$ inhibition prolongs the cardiac action potential duration and increases calcium transient and contractile amplitude. (a) (i) Representative traces of ventricular cardiomyocyte action potentials in the absence (control) or presence of either 3 μM PNU or 10 μM glibenclamide. (ii) Bar chart showing the mean change in APD_{90} by PNU37883A (PNU) or glibenclamide from control (*P<0.05, repeated-measures ANOVA with Holm–Sidak's post-test, n = 5 animals [10 cells]). (b) Mean APD_{90} for control and *KCNJ8*-KD virus-treated cells (*P<0.05, unpaired *t* test, n = 11 animals [39 cells] in each dataset). (c) A Rudy–O'Hara-based CellML simulation of the human ventricular AP modified to contain both $K_{ir}6.1$ and $K_{ir}6.2$ K_{ATP} channels. Simulation of the application of 10 μM PNU to inhibit $K_{ir}6.1$ caused a prolongation of the APD_{90}. (d) Representative traces of calcium transients in presence and absence of 3 μM PNU. (e) Calcium transients a have a larger (i) area under the curve (AUC) and (ii) change in peak Fluo-4 signal, indicative of increased $[Ca^{2+}]_i$ (*P<0.05, paired *t* test, n = 12 animals). (f) Edge-detection measurements in presence and absence of 3 μM PNU. (g) Analysis shows that exposure to 3 μM PNU increases (i) AUC and (ii) contraction amplitude in isolated cardiomyocytes (*P<0.05, paired *t* test, n = 6 animals).

(Figure 2e,f). There was a significant APD shortening with 150 μM pinacidil (Figure 6a,b). In the computer model, we also demonstrated that there was a concentration-dependent effect of potentiation of the two $K_{ir}6$-containing currents with a small $K_{ir}6.1$-dependent shortening with 10 μM pinacidil-induced $K_{ir}6.1$ potentiation, and a more significant shortening with $K_{ir}6.2$ activation, with higher concentrations of pinacidil (Figure 6c). This was corroborated in rabbit ventricular myocytes (Figure S8). In our hands, 200 μM pinacidil evoked a whole-cell K_{ATP} current with contributions from both $K_{ir}6.1$ and $K_{ir}6.2$. To assess the effects of $K_{ir}6.1$ and $K_{ir}6.2$ individually on Ca^{2+} and contractile function in cardiomyocytes, 50 μM pinacidil was used to selectively potentiate $K_{ir}6.1$ while 200 μM was used to

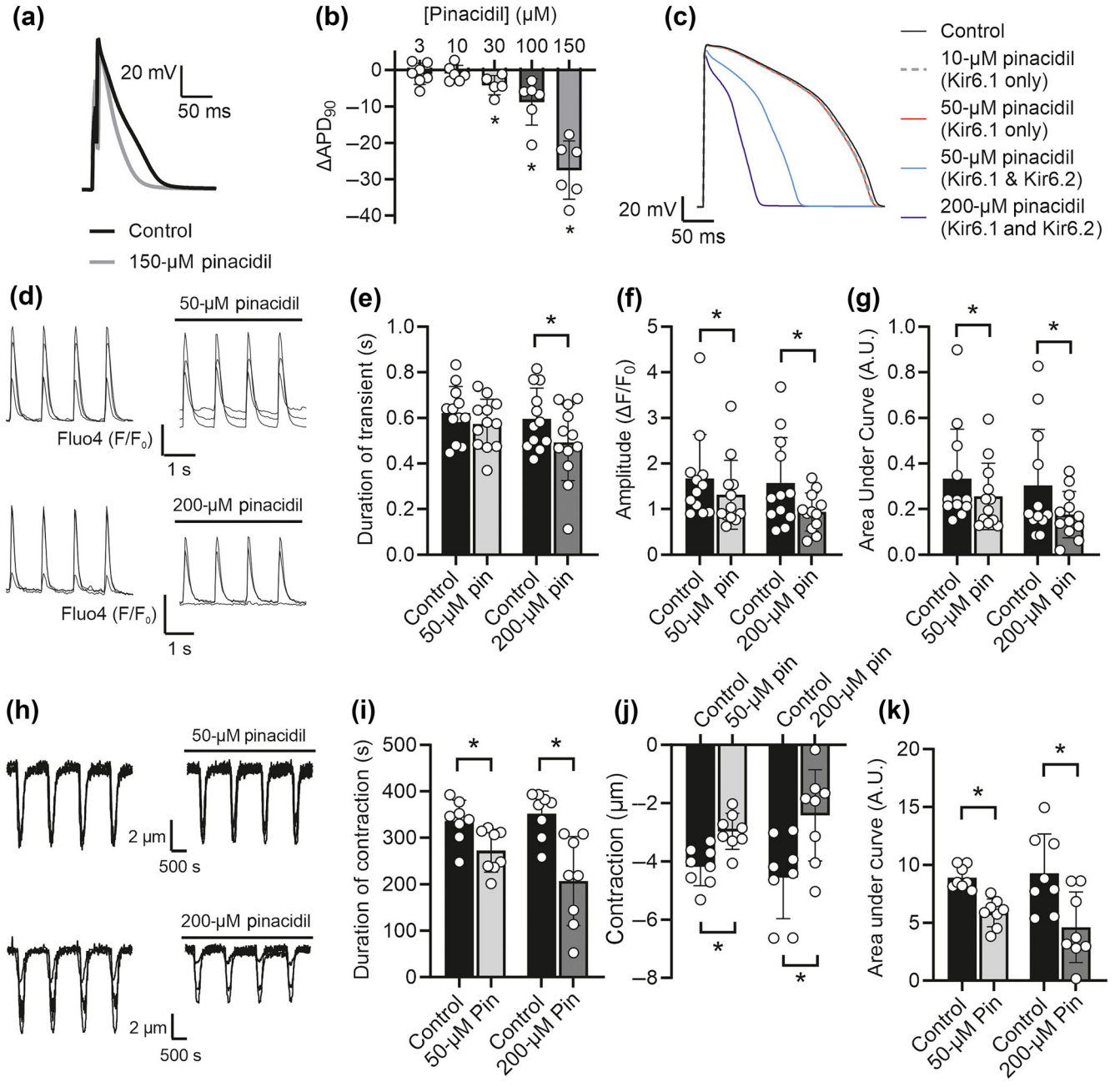

FIGURE 6 Direct $K_{ir}6.1$ activation shortens the cardiac action potential duration and reduces Ca^{2+} transient and contractile amplitude. (a) Example action potential traces in control and in perfusion with Tyrode's solution containing 150 μM pinacidil. (b) Bar chart showing the mean change in action potential duration (APD) APD_{90} from control with increasing concentrations of pinacidil (*P<0.05, repeated measures ANOVA, with Dunnett's posttest, n > 5 animals per pinacidil concentration, one to two concentrations of pinacidil applied to each cell). (c) A Rudy–O'Hara-based CellML simulation with the effects of pinacidil activation modelled in the activation of the two $K_{ir}6$ channels. Activation of solely $K_{ir}6.1$ resulted in a shorter APD_{90}, while this was further enhanced when the effects of pinacidil on $K_{ir}6.2$ were also modelled (note that 10 and 50 μM pinacidil [$K_{ir}6.1$ only] data are near identical and so overlay on the example trace). (d) Representative traces of cardiomyocyte Ca^{2+} transients recorded using fluo-4 in the absence and presence of 50- (top) or 200 μM pinacidil (bottom). Bar charts show (e) the changes in duration of transients, (f) amplitude of the transient (change in F/F_0) and (g) area under the curve (AUC) (*P<0.05, paired *t* test between control and following 5-min perfusion with pinacidil, n = 12 animals for each data set). (h) Representative traces of video edge-detection measurements from cardiomyocytes in the absence and presence of 50- (top) or 200 μM pinacidil (bottom). Bar charts show the (i) mean change in duration of contraction, (j) the change in amplitude of contraction and (k) the AUC (*P<0.05, Paired *t*-test between control and following 5 min perfusion with each pinacidil concentration, n = 8 animals for each data set).

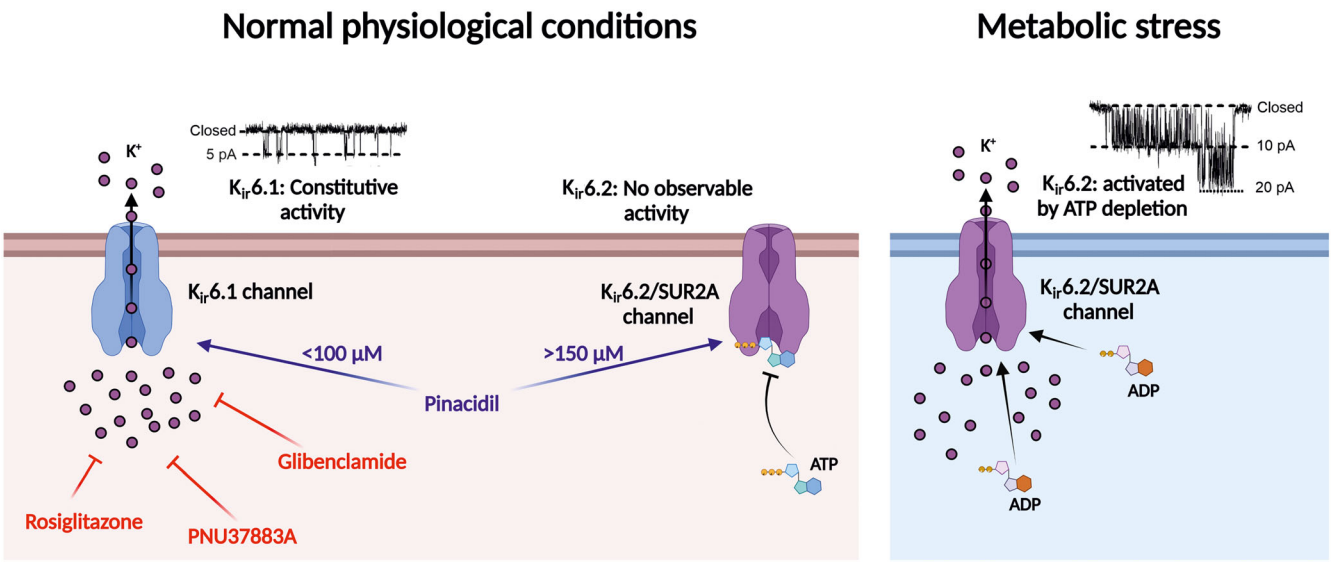

FIGURE 7 Illustrative figure of the proposed activities of the two distinct populations of $K_{ir}6$ channels at the ventricular cardiomyocyte cell membrane. Graphic created with BioRender.com.

additionally activate $K_{ir}6.2$/SUR2A. With 50 µM pinacidil, there was a smaller Ca^{2+} transient amplitude generated in response to electric field stimulation as hypothesised with a shorter APD (Figure 6d–g) and similar changes in contractile function (Figure 6h–k). Interestingly, in some cardiomyocytes treated with 200 µM pinacidil, there was a complete absence of Ca^{2+} transients in response to field stimulation (Figure S9A,B). These findings were also seen in contractile function measured by video edge detection, where some cardiomyocytes treated with 200 µM pinacidil showed complete contractile failure (Figure S9C,D). This is most likely indicative of the activation of $K_{ir}6.2$/SUR2A channels with the higher pinacidil concentration. Significant activation of this current would shorten the APD to such a degree that Ca^{2+}-influx and contraction is compromised.

4 | DISCUSSION AND CONCLUSIONS

In this report, we show that K^+ channels that are biophysically, pharmacologically and genetically identical to $K_{ir}6.1$-containing channels are expressed and constitutively active in the ventricular myocardium. We demonstrate that the current generated by these channels plays a role in fine-tuning the ventricular APD and thus influences both the size of the Ca^{2+} transient and contractile activity.

Forty years on from Noma's first description of the K_{ATP} channel in the heart (Noma, 1983), we still do not fully understand the role of these channels, despite their known property of matching electrical excitability to cellular metabolism. In the last decade, $K_{ir}6.1$ channels have been shown to regulate heart rate by altering the sinoatrial node APD (Aziz et al., 2018), and also coronary vasodilation (Aziz et al., 2014), due to the channel's expression in vascular smooth muscle. Here, we report a fundamental role for the Kir6.1-containing channel in the heart at the ventricular sarcolemmal surface where potentiation of the channel imparts action potential shortening and changes in Ca^{2+} homeostasis (Figure 7). This supports previous findings from multiple labs that have identified $K_{ir}6.1$ channel expression on the membrane surface (Morrissey, Parachuru, et al., 2005; Morrissey, Rosner, et al., 2005; Singh et al., 2003). This report does not rule out or support the existence of $K_{ir}6.1$ channels in the mitochondria; however, it does support a role for a sarcolemmal-$K_{ir}6.1$ channels under physiological conditions in ventricular myocytes.

K_{ATP} channel pharmacology in the heart is complicated by numerous reports identifying both proarrhythmic and antiarrhythmic effects of K_{ATP} channel openers and blockers (Brady & Terzic, 1998). During ischaemia, significant shortening of the APD caused by K_{ATP} channel activation can result in two contrasting consequences: (1) reduced Ca^{2+} influx via voltage-gated Ca^{2+} channels, resulting in a decreased arrhythmia risk from delayed after depolarisations, and (2) reduced refractoriness, resulting in an increased occurrence of re-entrant arrhythmias (Brady & Terzic, 1998). This report raises the possibility that perhaps only the canonical of the two sarco-K_{ATP} channels in cardiomyocytes ($K_{ir}6.2$/SUR2A), rather than all K_{ATP} channels, is mechanistically responsible for the reports of arrhythmias during ischaemia. This is a reasonable suggestion given the distinct properties of the two K_{ATP} channels at the ventricular membrane. $K_{ir}6.2$ channels, activated in high concentrations of pinacidil or metabolic poison, consequently cause a marked shortening of APD. This is comparable to the established effects of gain-of-function hERG mutations in short-QT, which cause arrhythmias via shortening of the APD and refractoriness (Brugada et al., 2004). In contrast, $K_{ir}6.1$ are constitutively active and provide subtle shortening of the action potential and so may not affect refractoriness. We infer, from the constitutive activity in normal physiological conditions, a relative ATP-insensitivity of these channels. Interestingly, key differences between global and vascular-specific $K_{ir}6.1$ knock-out could be explained by ventricular $K_{ir}6.1$ expression

(Aziz et al., 2014; Dart, 2014; Miki et al., 2002). Both global and vascular-specific K_{ir}6.1-KO mice are hypertensive, but global K_{ir}6.1 knockouts also display ST-elevation, indicative of acute myocardial ischaemia and are prone to sudden death. The lack of ST-elevation and sudden death in vascular-specific K_{ir}6.1 knockouts could be attributed to ventricular K_{ir}6.1 imparting a crucial modulatory role in the action potential and calcium handing of the myocardium. A limitation of the data presented in this study is that it is all based on rodent rather than human cardiomyocytes. Indeed, our computer model of the cardiac action potential, which is based on human data, showed a more modest change in APD compared to those recorded in rodent cardiomyocytes. This perhaps reflects a limitation in using rodent data to inform human cardiac models. It will be important to establish the functional expression levels of the K_{ir}6.1 component in human cardiomyocytes for future studies.

The pharmacology and kinetics of the newly identified cardiac channel is similar to published literature on K_{ir}6.1 channels in other tissue; however, care should be taken in comparing the responses of channels in different tissues as other proteins in the complex may lead to different kinetic properties. Furthermore, the identity of the SUR subunit coexpressed with this K_{ir}6.1 channels is yet to be determined. The data from CHO cells stably expressing K_{ir}6.1/SUR2B suggest that 10 μM pinacidil fully activates the K_{ir}6.1-pore; however, previous data from K_{ir}6.1 coexpressed with SUR2A shows that the EC_{50} for pinacidil is somewhat right shifted (∼45 μM) (Lodwick et al., 2014). As we do not currently know the SUR2 subunit that is coexpressed with the K_{ir}6.1 subunit, it is entirely plausible that there is a mixed population of K_{ir}6.1 with either SUR2A or 2B in ventricular myocytes. From our cell-attached data, it is clear, however, that we do not see K_{ir}6.2 activity below 150 μM pinacidil. The published IC_{50} concentrations for PNU37883A in K_{ir}6.1/SUR2B or vascular K_{ATP} channels (6 μM, Cui et al., 2003; 4.9 μM, Kovalev et al., 2004; 3.5 μM, Wellman et al., 1999) are not dissimilar to our own observations in this study (∼2 μM, depending on the configuration of recording). The similar glibenclamide efficacy (∼47 nM, and closely mimicked with Kir6.1/SUR2B expressed in CHO cells, ∼40 μM) and potentiation with pinacidil at concentrations analogous with that in smooth muscle lend further evidence to this being a K_{ir}6.1 channel. The inhibition of the K_{ir}6.1 channel by rosiglitazone, however, not by the related compound pioglitazone, is similar to findings by other groups further adding to the evidence of this channel being K_{ir}6.1. Finally, the kinetics of the channel activity observed in these cell-attached recordings was similar to those in HEK293 cells expressing K_{ir}6.1/SUR2B (Davies et al., 2010). Differences between these two studies, where the kinetics of the channel appear faster in the cell-attached data presented here, may be due to the HEK293 cell data in Davies et al. being recorded at room temperature, with this current study being at 32 ± 2°C. The selectivity of pharmacological modulators of K_{ATP} currents for the different K_{ir}6/SUR combinations appears to differ with expression system, tissue used and even the temperature at which the recording is made. When investigating K_{ATP} pharmacology in this study, we have endeavoured to use concentrations that are known to be as selective as possible for the channel subunit configuration under investigation while maintaining temperature consistent across all cellular recordings, where possible (Cui et al., 2003; Findlay, 1993; Kovalev et al., 2004; Rainbow et al., 2005; Sheppard & Welsh, 1992).

A role for this putative sarco-K_{ir}6.1 in the modulation of the action potential duration is supported by our current report. Although we believe that this newly identified Kir6.1 channel is relatively ATP-insensitive, given that it is active in normal physiological conditions, we have not investigated a role for this channel during metabolic compromise. Further study of this channel, in both physiological and ischaemic conditions, will be required to determine whether selective K_{ir}6.1 modulation could be a novel therapeutic target for the treatment of acute coronary syndromes, arrhythmias, and reversal of drug-induced long-QT syndrome, or whether this is an overlooked target in Comprehensive in vitro Proarrhythmia Assay (CiPA) cardiac safety screens. The presence of this channel in cardiomyocytes isolated from multiple different species, including rat, mouse, guinea pig, rabbit and pig cardiomyocytes, gives us a good indication that there is at least functional expression of this isoform at the sarcolemmal membrane of all of these species. The NP_O recorded from the channels in each species, however, did vary, and so future work is required to assess the relative contribution of this channel to the membrane currents in the different species.

This study shows that there are two functionally-distinct populations of K_{ATP} channel located at the sarcolemma of cardiomyocytes: (1) constitutively active Kir6.1-containing channels that provide a modulatory role on the action potential and so on Ca^{2+} handling during excitation-contraction coupling and (2) the canonical K_{ir}6.2/SUR2A channels that activate only after prolonged ischaemia to impart late-stage protection against catastrophic ATP depletion (Figure 7). The opening of this, larger conductance, K_{ir}6.2/SUR2A complex is enough to cause complete action potential failure as an energy-sparing protective process. The finding of a constitutively active K_{ir}6.1-containing population of K_{ATP} channels in cardiomyocytes provides an explanation to the paradox that K_{ATP} channel activation is cardioprotective; however, activation of the known cardiac isoform, K_{ir}6.2/SUR2A, is delayed in cardioprotected cells (Brennan et al., 2015). We present data that show that in cardiomyocytes, increases in the constitutive activity of K_{ir}6.1-containing channels lead to a modest shortening of the APD_{90} and reduced intracellular Ca^{2+} levels.

This study suggests that K_{ir}6.1 has a constitutive activity in ventricular cardiomyocytes that 'fine tunes' action potential duration in normal physiological conditions. Prolonged ischaemia will result in a collapse of intracellular ATP levels and the opening of canonical K_{ir}6.2/SUR2A channels as an energy-sparing last-line-of-defence, providing distinct physiological/pathophysiological roles for these two members of the K_{ir}6 family.

AUTHOR CONTRIBUTIONS

Investigation and formal analysis: S. Brennan, S. Chen, S. Makwana, S. Esposito, L. R. McGuinness, A. I. M. Alnaimi, M. W. Sims, M. Patel, Q. Aziz, L. Ojake, J. A. Roberts, P. Sharma, R. Barrett-Jolley, R. D. Rainbow. *Funding acquisition and supervision*: S. Brennan, C. Dart, R. D. Rainbow. *Methodology*: S. Brennan, Q. Aziz, P. Sharma, D. Lodwick,

A. Tinker, R. Barrett-Jolley, C. Dart, R. D. Rainbow. *Project administration*: A. Tinker, R. Barrett-Jolley, C. Dart, R. D. Rainbow. *Writing—original draft*: S. Brennan, C. Dart, R. D. Rainbow. *Writing—review and editing*: S. Brennan, Q. Aziz, P. Sharma, D. Lodwick, A. Tinker, R. Barrett-Jolley, C. Dart, R. D. Rainbow.

ACKNOWLEDGEMENTS

We acknowledge support from the British Heart Foundation (PG/16/14/32039 [SB, CD and RDR], PG/19/18/34280 [SB and RDR] and FS/PhD/21/29165 [LRM and RDR]). This work was also supported by an internal funding scheme funded by the Wellcome Trust Institutional Strategic Support Fund grant (204822/Z/16/Z) and awarded to SB and RDR by the Faculty of Health and Life Sciences, University of Liverpool. This study was also supported by the University of Leicester (RDR, SB, SC, MWS, SE, SM, and CWM).

CONFLICT OF INTEREST STATEMENT

None.

DATA AVAILABILITY STATEMENT

The data that support the findings of this study are available from the corresponding author upon reasonable request.

DECLARATION OF TRANSPARENCY AND SCIENTIFIC RIGOUR

This Declaration acknowledges that this paper adheres to the principles for transparent reporting and scientific rigour of preclinical research as stated in the *BJP* guidelines for Design and Analysis, and Animal Experimentation, and as recommended by funding agencies, publishers and other organisations engaged with supporting research.

ORCID

Richard Barrett-Jolley https://orcid.org/0000-0003-0449-9972
Richard D. Rainbow https://orcid.org/0000-0002-0532-1992

REFERENCES

Aguilar-Bryan, L., Clement, J. P. t., Gonzalez, G., Kunjilwar, K., Babenko, A., & Bryan, J. (1998). Toward understanding the assembly and structure of KATP channels. *Physiological Reviews*, *78*(1), 227–245. https://doi.org/10.1152/physrev.1998.78.1.227

Aguilar-Bryan, L., Nichols, C. G., Wechsler, S. W., Clement, J. P. t., Boyd, A. E. 3rd, González, G., Herrera-Sosa, H., Nguy, K., Bryan, J., & Nelson, D. A. (1995). Cloning of the beta cell high-affinity sulfonylurea receptor: A regulator of insulin secretion. *Science*, *268*(5209), 423–426. https://doi.org/10.1126/science.7716547

Akrouh, A., Halcomb, S. E., Nichols, C. G., & Sala-Rabanal, M. (2009). Molecular biology of K (ATP) channels and implications for health and disease. *IUBMB Life*, *61*(10), 971–978. https://doi.org/10.1002/iub.246

Alexander, S. P. H., Fabbro, D., Kelly, E., et al. (2023). The Concise Guide to PHARMACOLOGY 2023/24: Transporters. *Br J Pharmacol*, *180*, S374–S469. https://doi.org/10.1111/bph.16182

Alexander, S. P. H., Mathie, A. A., Peters, J. A., et al. (2023). The Concise Guide to PHARMACOLOGY 2023/24: Ion channels. *Br J Pharmacol*, *180*, S145–S222. https://doi.org/10.1111/bph.16181

Aziz, Q., Finlay, M., Montaigne, D., Ojake, L., Li, Y., Anderson, N., Ludwig, A., & Tinker, A. (2018). ATP-sensitive potassium channels in the sinoatrial node contribute to heart rate control and adaptation to hypoxia. *Journal of Biological Chemistry*, *293*, 8912–8921. https://doi.org/10.1074/jbc.RA118.002775

Aziz, Q., Li, Y., Anderson, N., Ojake, L., Tsisanova, E., & Tinker, A. (2017). Molecular and functional characterization of the endothelial ATP-sensitive potassium channel. *The Journal of Biological Chemistry*, *292*(43), 17587–17597. https://doi.org/10.1074/jbc.M117.810325

Aziz, Q., Thomas, A. M., Gomes, J., Ang, R., Sones, W. R., Li, Y., … Tinker, A. (2014). The ATP-sensitive potassium channel subunit, Kir6.1, in vascular smooth muscle plays a major role in blood pressure control. *Hypertension*, *64*(3), 523–529. https://doi.org/10.1161/HYPERTENSIONAHA.114.03116

Beech, D. J., Zhang, H., Nakao, K., & Bolton, T. B. (1993a). K channel activation by nucleotide diphosphates and its inhibition by glibenclamide in vascular smooth muscle cells. *British Journal of Pharmacology*, *110*(2), 573–582. https://doi.org/10.1111/j.1476-5381.1993.tb13849.x

Beech, D. J., Zhang, H., Nakao, K., & Bolton, T. B. (1993b). Single channel and whole-cell K-currents evoked by levcromakalim in smooth muscle cells from the rabbit portal vein. *British Journal of Pharmacology*, *110*(2), 583–590. https://doi.org/10.1111/j.1476-5381.1993.tb13850.x

Blenck, C. L., Harvey, P. A., Reckelhoff, J. F., & Leinwand, L. A. (2016). The importance of biological sex and estrogen in rodent models of cardiovascular health and disease. *Circulation Research*, *118*(8), 1294–1312. https://doi.org/10.1161/CIRCRESAHA.116.307509

Brady, P. A., & Terzic, A. (1998). The sulfonylurea controversy: More questions from the heart. *Journal of the American College of Cardiology*, *31*, 950–956. https://doi.org/10.1016/S0735-1097(98)00038-2

Brennan, S., Chen, S., Makwana, S., Martin, C. A., Sims, M. W., Alonazi, A. S. A., Willets, J. M., Squire, I. B., & Rainbow, R. D. (2019). A novel form of glycolytic metabolism-dependent cardioprotection revealed by PKCalpha and beta inhibition. *The Journal of Physiology*, *597*(17), 4481–4501. https://doi.org/10.1113/JP278332

Brennan, S., Jackson, R., Patel, M., Sims, M. W., Hudman, D., Norman, R. I., Lodwick, D., & Rainbow, R. D. (2015). Early opening of sarcolemmal ATP-sensitive potassium channels is not a key step in PKC-mediated cardioprotection. *Journal of Molecular and Cellular Cardiology*, *79*, 42–53. https://doi.org/10.1016/j.yjmcc.2014.10.016

Brennan, S., Rubaiy, H. N., Imanzadeh, S., Reid, R., Lodwick, D., Norman, R. I., & Rainbow, R. D. (2020). Kir6.2-D323 and SUR2A-Q1336: An intersubunit interaction pairing for allosteric information transfer in the KATP channel complex. *The Biochemical Journal*, *477*(3), 671–689. https://doi.org/10.1042/BCJ20190753

Brochiero, E., Wallendorf, B., Gagnon, D., Laprade, R., & Lapointe, J. Y. (2002). Cloning of rabbit Kir6.1, SUR2A, and SUR2B: Possible candidates for a renal K (ATP) channel. *American Journal of Physiology. Renal Physiology*, *282*(2), F289–F300. https://doi.org/10.1152/ajprenal.00063.2001

Brugada, R., Hong, K., Dumaine, R., Cordeiro, J., Gaita, F., Borggrefe, M., Menendez, T. M., Brugada, J., Pollevick, G. D., Wolpert, C., Burashnikov, E., Matsuo, K., Sheng Wu, Y., Guerchicoff, A., Bianchi, F., Giustetto, C., Schimpf, R., Brugada, P., & Antzelevitch, C. (2004). Sudden death associated with short-QT syndrome linked to mutations in HERG. *Circulation*, *109*(1), 30–35. https://doi.org/10.1161/01.CIR.0000109482.92774.3A

Chang, K. C., Dutta, S., Mirams, G. R., Beattie, K. A., Sheng, J., Tran, P. N., Wu, M., Wu, W. W., Colatsky, T., Strauss, D. G., & Li, Z. (2017). Uncertainty quantification reveals the importance of data variability and experimental design considerations for in silico proarrhythmia risk

assessment. *Frontiers in Physiology*, *8*, 917. https://doi.org/10.3389/fphys.2017.00917

Chicco, A. J., Johnson, M. S., Armstrong, C. J., Lynch, J. M., Gardner, R. T., Fasen, G. S., Gillenwater, C. P., & Moore, R. L. (2007). Sex-specific and exercise-acquired cardioprotection is abolished by sarcolemmal KATP channel blockade in the rat heart. *American Journal of Physiology. Heart and Circulatory Physiology*, *292*(5), H2432–H2437. https://doi.org/10.1152/ajpheart.01301.2006

Chutkow, W. A., Simon, M. C., Le Beau, M. M., & Burant, C. F. (1996). Cloning, tissue expression, and chromosomal localization of SUR2, the putative drug-binding subunit of cardiac, skeletal muscle, and vascular KATP channels. *Diabetes*, *45*(10), 1439–1445. https://doi.org/10.2337/diab.45.10.1439

Cole, W. C., McPherson, C. D., & Sontag, D. (1991). ATP-regulated K+ channels protect the myocardium against ischemia/reperfusion damage. *Circulation Research*, *69*(3), 571–581. https://doi.org/10.1161/01.res.69.3.571

Cui, Y., Giblin, J. P., Clapp, L. H., & Tinker, A. (2001). A mechanism for ATP-sensitive potassium channel diversity: Functional coassembly of two pore-forming subunits. *Proceedings of the National Academy of Sciences of the United States of America*, *98*(2), 729–734. https://doi.org/10.1073/pnas.011370498

Cui, Y., Tinker, A., & Clapp, L. H. (2003). Different molecular sites of action for the KATP channel inhibitors, PNU-99963 and PNU-37883A. *British Journal of Pharmacology*, *139*(1), 122–128. https://doi.org/10.1038/sj.bjp.0705228

Curtis, M. J., Alexander, S. P. H., Cirino, G., George, C. H., Kendall, D. A., Insel, P. A., Izzo, A. A., Ji, Y., Panettieri, R. A., Patel, H. H., Sobey, C. G., Stanford, S. C., Stanley, P., Stefanska, B., Stephens, G. J., Teixeira, M. M., Vergnolle, N., & Ahluwalia, A. (2022). Planning experiments: Updated guidance on experimental design and analysis and their reporting III. *British Journal of Pharmacology*, *179*(15), 1–7. https://doi.org/10.1111/bph.15868

D'Souza, A., Bucchi, A., Johnsen, A. B., Logantha, S. J., Monfredi, O., Yanni, J., Prehar, S., Hart, G., Cartwright, E., Wisloff, U., Dobryznski, H., DiFrancesco, D., Morris, G. M., & Boyett, M. R. (2014). Exercise training reduces resting heart rate via downregulation of the funny channel HCN4. *Nature Communications*, *5*, 3775. https://doi.org/10.1038/ncomms4775

Dart, C. (2014). Verdict in the smooth muscle KATP channel case: Guilty of blood pressure control but innocent of sudden death phenotype. *Hypertension*, *64*(3), 457–458. https://doi.org/10.1161/HYPERTENSIONAHA.114.03289

Davies, L. M., Purves, G. I., Barrett-Jolley, R., & Dart, C. (2010). Interaction with caveolin-1 modulates vascular ATP-sensitive potassium (KATP) channel activity. *The Journal of Physiology*, *588*(Pt 17), 3255–3266. https://doi.org/10.1113/jphysiol.2010.194779

Dutta, S., Chang, K. C., Beattie, K. A., Sheng, J., Tran, P. N., Wu, W. W., Wu, M., Strauss, D. G., Colatsky, T., & Li, Z. (2017). Optimization of an in silico cardiac cell model for proarrhythmia risk assessment. *Frontiers in Physiology*, *8*, 616. https://doi.org/10.3389/fphys.2017.00616

Fan, Z., Nakayama, K., & Hiraoka, M. (1990). Multiple actions of pinacidil on adenosine triphosphate-sensitive potassium channels in guinea-pig ventricular myocytes. *The Journal of Physiology*, *430*, 273–295. https://doi.org/10.1113/jphysiol.1990.sp018291

Findlay, I. (1993). Sulphonylurea drugs no longer inhibit ATP-sensitive K+ channels during metabolic stress in cardiac muscle. *The Journal of Pharmacology and Experimental Therapeutics*, *266*(1), 456–467. Retrieved from https://www.ncbi.nlm.nih.gov/pubmed/8331572

Flagg, T. P., Kurata, H. T., Masia, R., Caputa, G., Magnuson, M. A., Lefer, D. J., Coetzee, W. A., & Nichols, C. G. (2008). Differential structure of atrial and ventricular KATP: Atrial KATP channels require SUR1. *Circulation Research*, *103*(12), 1458–1465. https://doi.org/10.1161/CIRCRESAHA.108.178186

Han, X., Light, P. E., Giles, W. R., & French, R. J. (1996). Identification and properties of an ATP-sensitive K+ current in rabbit sino-atrial node pacemaker cells. *The Journal of Physiology*, *490*(Pt 2), 337–350. https://doi.org/10.1113/jphysiol.1996.sp021148

Hayabuchi, Y., Dart, C., & Standen, N. B. (2001). Evidence for involvement of A-kinase anchoring protein in activation of rat arterial K (ATP) channels by protein kinase a. *The Journal of Physiology*, *536*(Pt 2), 421–427. https://doi.org/10.1111/j.1469-7793.2001.0421c.xd

Hayabuchi, Y., Davies, N. W., & Standen, N. B. (2001). Angiotensin II inhibits rat arterial KATP channels by inhibiting steady-state protein kinase A activity and activating protein kinase Ce. *The Journal of Physiology*, *530*(Pt 2), 193–205. https://doi.org/10.1111/j.1469-7793.2001.0193l.x

He, T. C., Zhou, S., da Costa, L. T., Yu, J., Kinzler, K. W., & Vogelstein, B. (1998). A simplified system for generating recombinant adenoviruses. *Proceedings of the National Academy of Sciences of the United States of America*, *95*(5), 2509–2514. https://doi.org/10.1073/pnas.95.5.2509

Inagaki, N., Gonoi, T., Clement, J. P., Wang, C. Z., Aguilar-Bryan, L., Bryan, J., & Seino, S. (1996). A family of sulfonylurea receptors determines the pharmacological properties of ATP-sensitive K+ channels. *Neuron*, *16*(5), 1011–1017. https://doi.org/10.1016/s0896-6273(00)80124-5

Inagaki, N., Gonoi, T., Clement, J. P. t., Namba, N., Inazawa, J., Gonzalez, G., Aguilar-Bryan, L., Seino, S., & Bryan, J. (1995). Reconstitution of IKATP: An inward rectifier subunit plus the sulfonylurea receptor. *Science*, *270*(5239), 1166–1170. https://doi.org/10.1126/science.270.5239.1166

Inagaki, N., Tsuura, Y., Namba, N., Masuda, K., Gonoi, T., Horie, M., Seino, Y., Mizuta, M., & Seino, S. (1995). Cloning and functional characterization of a novel ATP-sensitive potassium channel ubiquitously expressed in rat tissues, including pancreatic islets, pituitary, skeletal muscle, and heart. *The Journal of Biological Chemistry*, *270*(11), 5691–5694. https://doi.org/10.1074/jbc.270.11.5691

Kono, Y., Horie, M., Takano, M., Otani, H., Xie, L. H., Akao, M., Tsuji, K., & Sasayama, S. (2000). The properties of the Kir6.1–6.2 tandem channel co-expressed with SUR2A. *Pflügers Archiv*, *440*(5), 692–698. https://doi.org/10.1007/s004240000315

Kovalev, H., Quayle, J. M., Kamishima, T., & Lodwick, D. (2004). Molecular analysis of the subtype-selective inhibition of cloned KATP channels by PNU-37883A. *British Journal of Pharmacology*, *141*(5), 867–873. https://doi.org/10.1038/sj.bjp.0705670

Li, N., Wu, J. X., Ding, D., Cheng, J., Gao, N., & Chen, L. (2017). Structure of a pancreatic ATP-sensitive potassium channel. *Cell*, *168*(1–2), 101–110 e110. https://doi.org/10.1016/j.cell.2016.12.028

Li, Z., Dutta, S., Sheng, J., Tran, P. N., Wu, W., Chang, K., Mdluli, T., Strauss, D. G., & Colatsky, T. (2017). Improving the in silico assessment of proarrhythmia risk by combining hERG (human ether-a-go-go-related gene) channel-drug binding kinetics and multichannel pharmacology. *Circulation. Arrhythmia and Electrophysiology*, *10*(2), e004628. https://doi.org/10.1161/CIRCEP.116.004628

Lilley, E., Stanford, S. C., Kendall, D. E., Alexander, S. P., Cirino, G., Docherty, J. R., George, C. H., Insel, P. A., Izzo, A. A., Ji, Y., Panettieri, R. A., Sobey, C. G., Stefanska, B., Stephens, G., Teixeira, M., & Ahluwalia, A. (2020). ARRIVE 2.0 and the *British Journal of Pharmacology*: Updated guidance for 2020. *British Journal of Pharmacology*, 177(16), 3611–3616. https://bpspubs.onlinelibrary.wiley.com/doi/full/10.1111/bph.15178

Lodwick, D., Rainbow, R. D., Rubaiy, H. N., Al Johi, M., Vuister, G. W., & Norman, R. I. (2014). Sulfonylurea receptors regulate the channel pore in ATP-sensitive potassium channels via an intersubunit salt bridge. *The Biochemical Journal*, *464*(3), 343–354. https://doi.org/10.1042/BJ20140273

Manning Fox, J. E., Kanji, H. D., French, R. J., & Light, P. E. (2002). Cardioselectivity of the sulphonylurea HMR 1098: Studies on native and

recombinant cardiac and pancreatic K (ATP) channels. *British Journal of Pharmacology*, *135*(2), 480–488. https://doi.org/10.1038/sj.bjp.0704455

Martin, G. M., Yoshioka, C., Rex, E. A., Fay, J. F., Xie, Q., Whorton, M. R., Chen, J. Z., & Shyng, S. L. (2017). Cryo-EM structure of the ATP-sensitive potassium channel illuminates mechanisms of assembly and gating. *eLife*, *6*, e24149. https://doi.org/10.7554/eLife.24149

Matsuoka, S., Sarai, N., Kuratomi, S., Ono, K., & Noma, A. (2003). Role of individual ionic current systems in ventricular cells hypothesized by a model study. *The Japanese Journal of Physiology*, *53*(2), 105–123. https://doi.org/10.2170/jjphysiol.53.105

Miki, T., Suzuki, M., Shibasaki, T., Uemura, H., Sato, T., Yamaguchi, K., Koseki, H., Iwanaga, T., Nakaya, H., & Seino, S. (2002). Mouse model of Prinzmetal angina by disruption of the inward rectifier Kir6.1. *Nature Medicine*, *8*(5), 466–472. https://doi.org/10.1038/nm0502-466

Morrissey, A., Parachuru, L., Leung, M., Lopez, G., Nakamura, T. Y., Tong, X., Yoshida, H., Srivastiva, S., Chowdhury, P. D., Artman, M., & Coetzee, W. A. (2005). Expression of ATP-sensitive K+ channel subunits during perinatal maturation in the mouse heart. *Pediatric Research*, *58*(2), 185–192. https://doi.org/10.1203/01.PDR.0000169967.83576.CB

Morrissey, A., Rosner, E., Lanning, J., Parachuru, L., Dhar Chowdhury, P., Han, S., Lopez, G., Tong, X., Yoshida, H., Nakamura, T. Y., Artman, M., Giblin, J. P., Tinker, A., & Coetzee, W. A. (2005). Immunolocalization of KATP channel subunits in mouse and rat cardiac myocytes and the coronary vasculature. *BMC Physiology*, *5*(1), 1. https://doi.org/10.1186/1472-6793-5-1

Nakayama, K., Fan, Z., Marumo, F., & Hiraoka, M. (1990). Interrelation between pinacidil and intracellular ATP concentrations on activation of the ATP-sensitive K+ current in guinea pig ventricular myocytes. *Circulation Research*, *67*(5), 1124–1133. https://doi.org/10.1161/01.res.67.5.1124

Nichols, C. G. (2006). KATP channels as molecular sensors of cellular metabolism. *Nature*, *440*(7083), 470–476. https://doi.org/10.1038/nature04711

Nichols, C. G. (2016). Adenosine triphosphate-sensitive potassium currents in heart disease and cardioprotection. *Cardiac Electrophysiology Clinics*, *8*(2), 323–335. https://doi.org/10.1016/j.ccep.2016.01.005

Noma, A. (1983). ATP-regulated K+ channels in cardiac muscle. *Nature*, *305*(5930), 147–148. https://doi.org/10.1038/305147a0

O'Hara, T., Virag, L., Varro, A., & Rudy, Y. (2011). Simulation of the undiseased human cardiac ventricular action potential: Model formulation and experimental validation. *PLoS Computational Biology*, *7*(5), e1002061. https://doi.org/10.1371/journal.pcbi.1002061

Percie du Sert, N., Hurst, V., Ahluwalia, A., Alam, S., Avey, M. T., Baker, M., Browne, W. J., Clark, A., Cuthill, I. C., Dirnagl, U., Emerson, M., Garner, P., Holgate, S. T., Howells, D. W., Karp, N. A., Lazic, S. E., Lidster, K., MacCallum, C. J., Macleod, M., … Würbel, H. (2020). The ARRIVE guidelines 2.0: Updated guidelines for reporting animal research. *PLoS Biology*, *18*(7), e3000410. https://doi.org/10.1371/journal.pbio.3000410

Qin, F. (2004). Restoration of single-channel currents using the segmental k-means method based on hidden Markov modeling. *Biophysical Journal*, *86*(3), 1488–1501. https://doi.org/10.1016/S0006-3495(04)74217-4

Quayle, J. M., McCarron, J. G., Brayden, J. E., & Nelson, M. T. (1993). Inward rectifier K+ currents in smooth muscle cells from rat resistance-sized cerebral arteries. *The American Journal of Physiology*, *265*(5 Pt 1), C1363–C1370. https://doi.org/10.1152/ajpcell.1993.265.5.C1363

Rainbow, R. D., Hardy, M. E., Standen, N. B., & Davies, N. W. (2006). Glucose reduces endothelin inhibition of voltage-gated potassium channels in rat arterial smooth muscle cells. *The Journal of Physiology*, *575*(Pt 3), 833–844. https://doi.org/10.1113/jphysiol.2006.114009

Rainbow, R. D., James, M., Hudman, D., Johi, M. A. L., Singh, H., Watson, P. J., Ashmole, I., Davies, N. W., Lodwick, D., & Norman, R. I. (2004). Proximal C-terminal domain of sulphonylurea receptor 2A interacts with pore-forming Kir6 subunits in KATP channels. *The Biochemical Journal*, *379*(Pt 1), 173–181. https://doi.org/10.1042/BJ20031087

Rainbow, R. D., Lodwick, D., Hudman, D., Davies, N. W., Norman, R. I., & Standen, N. B. (2004). SUR2A C-terminal fragments reduce KATP currents and ischaemic tolerance of rat cardiac myocytes. *The Journal of Physiology*, *557*(Pt 3), 785–794. https://doi.org/10.1113/jphysiol.2004.061655

Rainbow, R. D., Norman, R. I., Hudman, D., Davies, N. W., & Standen, N. B. (2005). Reduced effectiveness of HMR 1098 in blocking cardiac sarcolemmal K (ATP) channels during metabolic stress. *Journal of Molecular and Cellular Cardiology*, *39*(4), 637–646. https://doi.org/10.1016/j.yjmcc.2005.06.017

Sampson, L. J., Hayabuchi, Y., Standen, N. B., & Dart, C. (2004). Caveolae localize protein kinase A signaling to arterial ATP-sensitive potassium channels. *Circulation Research*, *95*(10), 1012–1018. https://doi.org/10.1161/01.RES.0000148634.47095.ab

Seharaseyon, J., Sasaki, N., Ohler, A., Sato, T., Fraser, H., Johns, D. C., O'Rourke, B., & Marbán, E. (2000). Evidence against functional heteromultimerization of the KATP channel subunits Kir6.1 and Kir6.2. *The Journal of Biological Chemistry*, *275*(23), 17561–17565. https://doi.org/10.1074/jbc.275.23.17561

Sheppard, D. N., & Welsh, M. J. (1992). Effect of ATP-sensitive K+ channel regulators on cystic fibrosis transmembrane conductance regulator chloride currents. *The Journal of General Physiology*, *100*(4), 573–591. https://doi.org/10.1085/jgp.100.4.573

Sims, M. W., Winter, J., Brennan, S., Norman, R. I., Ng, G. A., Squire, I. B., & Rainbow, R. D. (2014). PKC-mediated toxicity of elevated glucose concentration on cardiomyocyte function. *American Journal of Physiology. Heart and Circulatory Physiology*, *307*(4), H587–H597. https://doi.org/10.1152/ajpheart.00894.2013

Singh, H., Hudman, D., Lawrence, C. L., Rainbow, R. D., Lodwick, D., & Norman, R. I. (2003). Distribution of Kir6.0 and SUR2 ATP-sensitive potassium channel subunits in isolated ventricular myocytes. *Journal of Molecular and Cellular Cardiology*, *35*(5), 445–459. https://doi.org/10.1016/s0022-2828(03)00041-5

Storey, N. M., Stratton, R. C., Rainbow, R. D., Standen, N. B., & Lodwick, D. (2013). Kir6.2 limits Ca(2+) overload and mitochondrial oscillations of ventricular myocytes in response to metabolic stress. *American Journal of Physiology. Heart and Circulatory Physiology*, *305*(10), H1508–H1518. https://doi.org/10.1152/ajpheart.00540.2013

Sung, M. W., Yang, Z., Driggers, C. M., Patton, B. L., Mostofian, B., Russo, J. D., Zuckerman, D. M., & Shyng, S. L. (2021). Vascular K (ATP) channel structural dynamics reveal regulatory mechanism by Mg-nucleotides. *Proceedings of the National Academy of Sciences of the United States of America*, *118*(44), e2109441118. https://doi.org/10.1073/pnas.2109441118

Suzuki, M., Sasaki, N., Miki, T., Sakamoto, N., Ohmoto-Sekine, Y., Tamagawa, M., Seino, S., Marbán, E., & Nakaya, H. (2002). Role of sarcolemmal KATP channels in cardioprotection against ischemia/reperfusion injury in mice. *Journal of Clinical Investigation*, *109*(4), 509–516. https://doi.org/10.1172/jci0214270

Takano, M., Xie, L. H., Otani, H., & Horie, M. (1998). Cytoplasmic terminus domains of Kir6.x confer different nucleotide-dependent gating on the ATP-sensitive K+ channel. *The Journal of Physiology*, *512*(Pt 2), 395–406. https://doi.org/10.1111/j.1469-7793.1998.395be.x

Teramoto, N. (2006). Pharmacological profile of U-37883A, a channel blocker of smooth muscle-type ATP-sensitive K channels. *Cardiovascular Drug Reviews*, *24*(1), 25–32. https://doi.org/10.1111/j.1527-3466.2006.00025.x

Tinker, A., Aziz, Q., Li, Y., & Specterman, M. (2018). ATP-sensitive potassium channels and their physiological and pathophysiological roles.

Comprehensive Physiology, *8*(4), 1463–1511. https://doi.org/10.1002/cphy.c170048

Tran, K., Loiselle, D. S., & Crampin, E. J. (2015). Regulation of cardiac cellular bioenergetics: Mechanisms and consequences. *Physiological Reports*, *3*(7), e12464. https://doi.org/10.14814/phy2.12464

Wellman, G. C., Barrett-Jolley, R., Koppel, H., Everitt, D., & Quayle, J. M. (1999). Inhibition of vascular K (ATP) channels by U-37883A: A comparison with cardiac and skeletal muscle. *British Journal of Pharmacology*, *128*(4), 909–916. https://doi.org/10.1038/sj.bjp.0702868

Yamada, M., Isomoto, S., Matsumoto, S., Kondo, C., Shindo, T., Horio, Y., & Kurachi, Y. (1997). Sulphonylurea receptor 2B and Kir6.1 form a sulphonylurea-sensitive but ATP-insensitive K+ channel. *The Journal of Physiology*, *499*(Pt 3), 715–720. https://doi.org/10.1113/jphysiol.1997.sp021963

Yu, L., Jin, X., Cui, N., Wu, Y., Shi, Z., Zhu, D., & Jiang, C. (2012). Rosiglitazone selectively inhibits K (ATP) channels by acting on the K (IR) 6 subunit. *British Journal of Pharmacology*, *167*(1), 26–36. https://doi.org/10.1111/j.1476-5381.2012.01934.x

Yu, L., Jin, X., Yang, Y., Cui, N., & Jiang, C. (2011). Rosiglitazone inhibits vascular KATP channels and coronary vasodilation produced by isoprenaline. *British Journal of Pharmacology*, *164*(8), 2064–2072. https://doi.org/10.1111/j.1476-5381.2011.01539.x

Zhang, H. L., & Bolton, T. B. (1996). Two types of ATP-sensitive potassium channels in rat portal vein smooth muscle cells. *British Journal of Pharmacology*, *118*(1), 105–114. https://doi.org/10.1111/j.1476-5381.1996.tb15372.x

SUPPORTING INFORMATION

Additional supporting information can be found online in the Supporting Information section at the end of this article.

How to cite this article: Brennan, S., Chen, S., Makwana, S., Esposito, S., McGuinness, L. R., Alnaimi, A. I. M., Sims, M. W., Patel, M., Aziz, Q., Ojake, L., Roberts, J. A., Sharma, P., Lodwick, D., Tinker, A., Barrett-Jolley, R., Dart, C., & Rainbow, R. D. (2024). Identification and characterisation of functional K_{ir}6.1-containing ATP-sensitive potassium channels in the cardiac ventricular sarcolemmal membrane. *British Journal of Pharmacology*, 1–21. https://doi.org/10.1111/bph.16390